

ELASTO-PLASTIC EVOLUTION OF SINGLE CRYSTALS DRIVEN BY DISLOCATION FLOW

THOMAS HUDSON AND FILIP RINDLER

ABSTRACT. This work introduces a model for large-strain, geometrically nonlinear elasto-plastic dynamics in single crystals. The key feature of our model is that the plastic dynamics are entirely driven by the movement of dislocations, that is, 1-dimensional topological defects in the crystal lattice. It is well known that glide motion of dislocations is the dominant microscopic mechanism for plastic deformation in many crystalline materials, most notably in metals. However, a comprehensive model linking dislocation dynamics to elasto-plastic evolution has been missing to date. We propose a geometric language, built on the novel concepts of space-time “slip trajectories” and the “crystal scaffold” to describe the movement of (discrete) dislocations and to couple this movement to plastic flow. The energetics and dissipation relationships in our model are derived from first principles drawing on the theories of crystal modeling, elasticity, and thermodynamics. The resulting force balances involve a new configurational stress tensor describing the forces acting against slip. In order to place our model into context, we further show that it recovers several laws that were known in special cases before, most notably the equation for the Peach–Koehler force (linearized configurational force) and the fact that the combination of all dislocations yields the curl of the plastic distortion field. Finally, we also include a brief discussion how a number of other effects, such as hardening, softening, dislocation climb, and coarse-graining, could be incorporated into our model.

DATE: September 21, 2021

1. INTRODUCTION

The modeling of large-strain elasto-plasticity poses many challenges and, despite its great practical importance, no fully satisfactory theory has emerged so far. We refer to [45, 46, 70, 73, 105] for recent expositions (and many historical references) as well as the original works [2, 3, 27, 38, 43, 59, 72, 77, 79, 85, 86, 88, 94, 104, 109] for some aspects of this vast field. Most of the existing models are phenomenological in nature and do not attempt to explain plastic distortion from its microscopic origins, but merely describe its macroscopic manifestation. However, at least in crystalline materials, the microscopic origins of plasticity are fairly well understood: Essentially all plastic distortion is caused by the movement of dislocations, that is, 1-dimensional topological defects in the crystal lattice [1, 9, 55]. For topological reasons, dislocations are always closed loops inside the crystal specimen, or, if the specimen is polycrystalline, inside a grain. Every dislocation line has associated with it a *Burgers vector*, which is fixed along the whole dislocation line and specifies the plastic displacement effected when the dislocation moves. The description of dislocations and their movement (in crystals) are considered for instance in the works [1, 7, 8, 15, 18, 26, 35, 47–49, 61, 63, 64, 66, 67, 100]. However, what has so far been missing is a theory that relates macroscopic plasticity in the large-strain regime to microscopic dislocation motion in a mechanically, thermodynamically, and mathematically satisfactory manner.

It is the goal of this work to derive such a rational model of elasto-plastic evolution driven by dislocation motion, based on explicit mechanical and thermodynamic axioms as well as a few well-established constitutive assumptions.

As in several other recent works [24, 25, 64, 101], we describe individual dislocations on a mesoscale as closed 1-dimensional loops in a 3-dimensional body occupying the reference (initial) configuration $\Omega \subset \mathbb{R}^3$. For the evolution of such a dislocation system we introduce the notion of a *slip trajectory*, that is, a 2-dimensional oriented surface S in the space-time cylinder $[0, T] \times \bar{\Omega}$. The dislocation at time t is then given as the *slice* $S|_t$ of S at time t , i.e. the intersection of S

with the plane $\{t\} \times \mathbb{R}^3$, which can be shown to be a collection of oriented lines; see Figure 5 for an illustration. The notion of a slip trajectory can be made mathematically rigorous using the theory of integral currents [37, 58], but we present the model with minimal technicalities, confining mathematical details to an appendix.

We believe that the use of slip trajectories is a key conceptual step for developing a well-posed mathematical theory of dislocation motion, and this point of view seems to be different from all existing works we are aware of, including numerous classical approaches [14, 59, 60, 62, 87]. In particular, it is distinct from the usual approach taken in the simulation methodology of Discrete Dislocation Dynamics [7, 8, 15, 106], where it is assumed that dislocation line segments can be assigned a pointwise velocity. There are several notable advantages of our approach: First, it allows to define the associated change in plastic distortion in a straightforward way. Second, there is a natural “geometric derivative” replacing the pointwise velocity of dislocation movement while containing more information. Third, working in a suitably general class of slip trajectories, we can evolve dislocations independently, even if they overlap or cross, which is not possible if considering “global” velocity fields (velocity fields “along the dislocation curves” require a parameterization, which is not readily available and also not preserved under the flow). As such, our approach provides a “weak formulation” of the dislocation motion, which we hope is sufficiently rich in structure to include all important physics and enable further rigorous analysis in the future.

Having outlined the description of dislocations in our model, we now turn to the connection between dislocation motion and the macroscopic mechanical properties of our specimen. Denoting the total deformation of our specimen as $y: \Omega \subset \mathbb{R}^3 \rightarrow \mathbb{R}^3$, for which $\det \nabla y > 0$, the commonly used *multiplicative* Kröner decomposition

$$\nabla y = EP$$

splits the deformation gradient into elastic and plastic distortions E, P . Since E, P are not in general deformation gradients themselves, they are henceforth referred to as “distortions”. We refer to [20, 35, 43, 45, 59, 63, 68, 69, 92, 93] for justifications and various other aspects of this decomposition. Our description of the crystal in Section 2.3 will in fact give its own justification of the Kröner decomposition based on the *crystal scaffold*, which is the variable we use to describe the state of the crystal around a point. Namely, the crystal scaffold describes the bonds between the lattice atoms relative to the referential positions of the atoms. It is a purely kinematic quantity and can be defined unambiguously (unlike P , whose definition contains some ambiguities, which have to be explicitly excluded). We refer to Figure 1 for a schematic overview of our model.

The elastic energy functional (assuming that our specimen is hyperelastic) only depends on E , i.e.,

$$\int_{\Omega} W_e(E) \, dx = \int_{\Omega} W_e(\nabla y P^{-1}) \, dx,$$

where W_e is the elastic energy density. Note that if P is fixed and not a gradient (i.e., $\text{curl } P \neq 0$), the material may not be able to elastically relax to a stress-free configuration, see [71, Theorem 2.2] and [63, Theorem 1.4]. In this sense, our “reference configuration” should only be understood as a fixing of spatial coordinates and not as a configuration with special properties.

Our approach considers the plastic distortion P to be an internal variable (like in [38, 74, 75, 79, 80]) and specifies that the evolution of P occurs via the *plastic flow equation*

$$\dot{P} = D \tag{1.1}$$

involving the *total plastic drift* D , which acts as an infinitesimal (microscopic) generator of the flow of P . This in particular removes all ambiguity in the Kröner decomposition in our model, since we require that P can change only through the motion of dislocations.

We propose that the plastic drift is expressed in terms of the movement of dislocations, i.e. via a slip trajectory. Namely, if a dislocation with Burgers vector b moves in space-time along a slip trajectory S , then $D(t)$ is the $\mathbb{R}^{3 \times 3}$ -valued measure (i.e., a “singular density”) on Ω given by

$$D(t) = b \otimes g^b \mathcal{H}^1 \llcorner S^b|_t, \tag{1.2}$$

where $S^b|_t$ is the slice of S at time t , i.e. the dislocation line at time t , $\mathcal{H}^1 \llcorner S^b|_t$ is the (Hausdorff-)measure concentrated on the dislocation line, and g^b is the *geometric slip rate*, which is given as

$$g^b := v^b \times \vec{T}^b,$$

that is, the vector cross product of the *dislocation velocity* $v^b \in \mathbb{R}^3$ and the dislocation line direction \vec{T}^b . Both v^b and \vec{T}^b can be obtained directly from S^b , but not from $S^b|_t$ alone (because the change in the time direction, i.e., the dislocation velocity, is missing). It therefore becomes clear that in order to define the plastic evolution we need to consider the complete *path* of plastic evolution between two given points in time. Merely considering the endpoints of “elementary” movements as in the rate-independent models of [38, 74, 75, 79, 80] does not give us access to this information.

With the kinematics and dynamics specified, we then apply two fundamental principles of energetic modeling in mechanics, namely the *Principle of Virtual Power* [45, Chapter 92] and the *Free Energy Imbalance* [45, Section 27.3], which is a consequence of the *Second Law of Thermodynamics*. This yields formulas for the stresses corresponding to elastic and plastic distortions as well as the *configurational stress* induced by dislocation motion. For the elastic and plastic stresses we recover (a version of) the classical Piola–Kirchhoff stress and the Mandel stress, respectively. For the configurational stress, that is, the stress power-conjugate to dislocations slip, we obtain an explicit expression, which is later seen to be a nonlinear analogue of the classical Peach–Koehler force.

The last ingredient of our model is a *flow rule*, i.e. the constitutive relationship between rates and stresses, on the level of dislocations. A version of this approach is already employed in the Engineering literature on discrete dislocation dynamics, where *mobilities* are typically prescribed [15]. Here, we additionally connect this viewpoint with a fully nonlinear and frame-indifferent nonlinear elasticity theory (which is not present in the existing models). With a flow rule prescribed, our model is closed.

Let us remark that at some points this work makes some use of the language of currents (and with this, the language of differential geometry). In particular, this is the case when considering 2-dimensional surfaces in 4-dimensional space-time, where classical vector analysis has shortcomings (namely, there is no vector cross product in \mathbb{R}^4). While this is unavoidable for being precise in dealing with geometric objects, we have aimed to keep this to the absolute minimum necessary.

In this vein, one could have employed the so-called “geometrical language of continuum mechanics” [22, 34, 35] to obtain an additional level of consistency (and, perhaps, elegance), but this brings with it further notational complications. We have therefore opted not to pursue this avenue here. One noteworthy point in this respect is that the dislocation density of continuously distributed (and grain-homogenized) dislocations can be identified with the torsion tensor of an affine material connection [35, 47, 57, 63–67, 76] (which can be seen as the limit of discrete dislocations [35, 63, 64]).

The present article does not aim to define all notions in a mathematically rigorous fashion and instead focuses on the physical modeling. However, we give some indication of how these notions can be made rigorous using the theory of integral currents in Appendix A. The actual mathematical implementation of the model is contained in two forthcoming works: First, the paper [96] develops a mathematical theory of space-time integral currents, which in our case represent the slip trajectories. In particular, the notion of “variation” (in time) is introduced and a number of results (e.g., on deformation, compactness, and comparison) are proved. Second, the work [95] proves an existence theorem for solutions to the rate-independent instance of our model, which can be interpreted as a validation of its mathematical consistency.

Outline. This manuscript is organized as follows: In Section 2, we present the kinematic framework for plastic distortions and dislocations. In Section 3, we discuss the dynamics of dislocations and the of the macroscopic body, and derive an equation connecting the two. Then in Section 4,

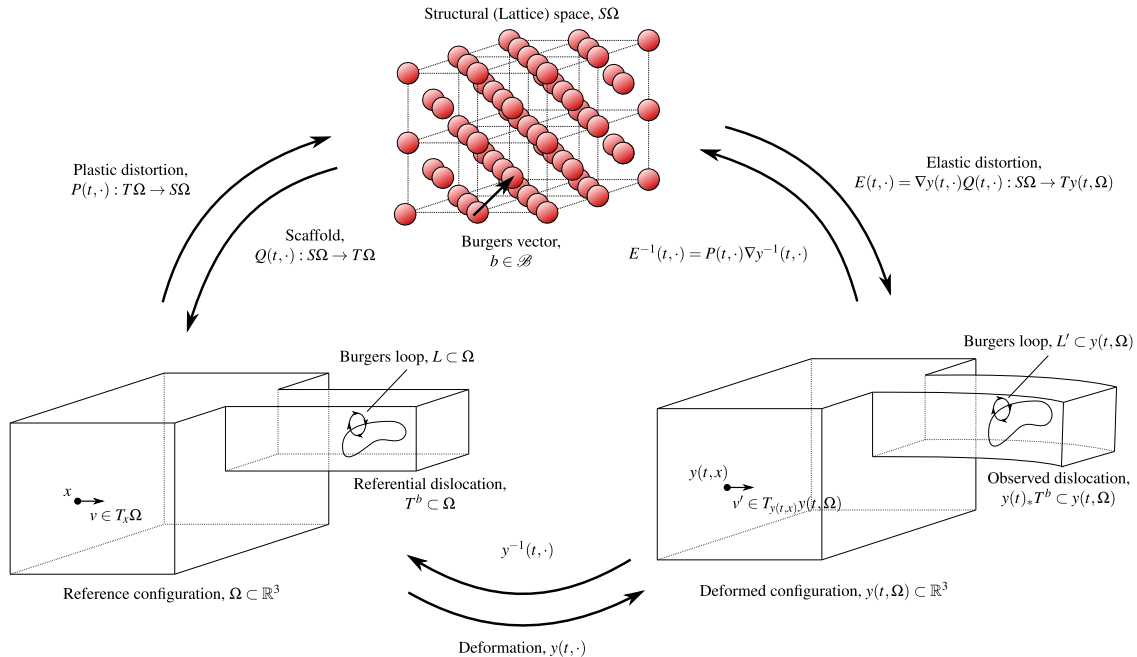


FIGURE 1. An overview of the kinematic framework.

we describe the energetic framework, within which we consider the evolution, and derive appropriate balance laws by applying fundamental thermodynamic principles. Section 5 summarizes all equations of the model. Finally, in Section 6, we present a discussion of various special cases of our model, our conclusions, and an outlook. Appendix A is devoted to describing some aspects of the rigorous geometric setting forming a more solid foundation for our model.

Acknowledgements. This project has received funding from the European Research Council (ERC) under the European Union’s Horizon 2020 research and innovation programme, grant agreement No 757254 (SINGULARITY). Some parts of this work appeared in [97] in preprint form. The authors would like to thank Gilles Francfort, Cy Maor, Marco Morandotti, and Michael Ortiz for helpful discussions related to the topic of this work.

2. KINEMATICS

In this section we describe our approach to the modeling of the elastic, plastic, and dislocation kinematics of our specimen; a pictorial overview of our framework is provided in Figure 1.

2.1. Basic modeling assumptions. We will consider a body formed of a single crystal, which will be allowed to be both elastically and plastically deformed. We state the fundamental principle of plasticity in crystalline materials as follows:

Plastic distortions manifest as changes to the crystal lattice, i.e. the breaking and reforming of bonds between the lattice atoms.

Along with the usual description of material deformation through notions of strain, we will consider the local configuration of bonds in the crystal as a form of *microstructure* attached to each material point. In particular, there are two important phenomena we keep track of:

- (i) **Slip**, i.e., the history of any rearrangement of interatomic bonds in the crystal.
- (ii) **Dislocations**, i.e., topological line defects in the crystal lattice, which cause a rearrangement of bonds to occur when they move through the material.

These two features are described by **internal variables**, that is, additional quantities indexed by time t and material points x . In particular, in agreement with experimental observation [9, 55], we will assume within our modeling framework that these two phenomena are connected:

Slip occurs (only) through the motion of dislocations.

We remark that focusing solely on these phenomena is valid as long as dislocations are relatively sparse and no other significant defects are present, such as a large number of point defects, grain boundaries, or cracks. Consideration of these lies beyond the remit of the present work.

2.2. Deformation. We start by fixing a Cartesian coordinate system on the 3-dimensional space within which the crystalline body is embedded; throughout this work, we will identify spatial points with their coordinate representation in \mathbb{R}^3 in this fixed coordinate frame. We then consider an open, bounded, connected **reference configuration** $\Omega \subset \mathbb{R}^3$ of material (or, more generally, a 3-dimensional Riemannian manifold Ω). We denote the **referential (Lagrange, material) points** in Ω as $x = (x^1, x^2, x^3)$. Under a **(total) deformation** $y = (y^1, y^2, y^3): \Omega \rightarrow \mathbb{R}^3$, every referential point x is mapped to a **spatial (Euler) point** $y = y(t, x) \in y(t, \Omega)$, where the time t is from an interval $[0, T]$. In the modeling that follows, we assume that y and all other quantities are as smooth as required and we will frequently suppress function arguments for ease of reading.

A fundamental modeling assumption in this work (as in the continuum theory of elasticity and plasticity in general) is the following:

Macroscopically, the deformed body is again a continuum without interpenetration of matter or holes, and it has the same orientation as the reference configuration.

In mathematical terms, this means that $y(t) = y(t, \cdot)$ is an orientation-preserving diffeomorphism, i.e., $y(t)$ is smooth, bijective, $\nabla y(t) \in \text{GL}^+(3)$, i.e., $\det \nabla y(t) > 0$ in Ω , and the inverse $y(t)^{-1}$ is itself smooth. Here, we denote the **(spatial) deformation gradient** as

$$\nabla y(t, x) = \left[\frac{\partial y^j}{\partial x^k}(t, x) \right]_k^j \in \mathbb{R}^{3 \times 3}.$$

We also remark at this point that derivatives with respect to the time variable t of the various fields we consider will be denoted using the dot notation, i.e., $\dot{y} = \frac{\partial}{\partial t} y$.

A **referential vector** $v \in T_x \Omega$ at a referential point $x \in \Omega$, where $T_x \Omega \cong \mathbb{R}^3$ denotes the tangent space to Ω at $x \in \Omega$, is transformed into an **observed (spatial) vector** $w \in T_{y(t, x)} y(t, \Omega)$ via the pushforward under y ,

$$w := \nabla y(t, x)v.$$

Physically, this is simply the statement that $\nabla y(t, x)$ encodes the net local transformation of the material close to a material point x at some time t . While higher-order measures of strain could be considered, we will make the usual assumption (see, e.g., [21]) that

The deformation gradient is sufficient to describe the strain in the body we consider.

2.3. Crystal scaffold and plastic distortion. We now introduce two ways to describe the slip that has taken place up to a time t at a referential point x , namely the plastic distortion P and the crystal scaffold Q . Heuristically, the former describes the rearrangement of the atoms in the lattice due to slip, while the latter describes the rearrangement of the bonds. Both descriptions are mathematically equivalent, but from a modeling perspective they emphasize different aspects, and once we have described both approaches, we will freely transition between them.

Let $\varepsilon > 0$ be the microscopic lattice length scale (viewed as infinitesimal relative to our macroscopic length scale) and fix a material (Lagrangian) point x , which is mapped to a spatial (Euler) point y by the deformation. For simplicity, suppose first that the underlying structure of the crystal is simply cubic with unit cell $[0, \varepsilon]^3$. In the perfect crystal structure, the vectors εe_1 , εe_2 and εe_3 therefore point to the nearest neighbor atoms in the lattice. Assume now that plastic slip has taken place, so that the crystal bonds have been rearranged, and the crystal cell has been elastically deformed. We denote the vector corresponding to the i 'th bond in the deformed configuration by εE_i (these are the ‘‘arrows’’ connecting the atom at y with the atoms that are bonded to it). Let us further assume that the atom that is now (after both slip and elastic deformation) at the position

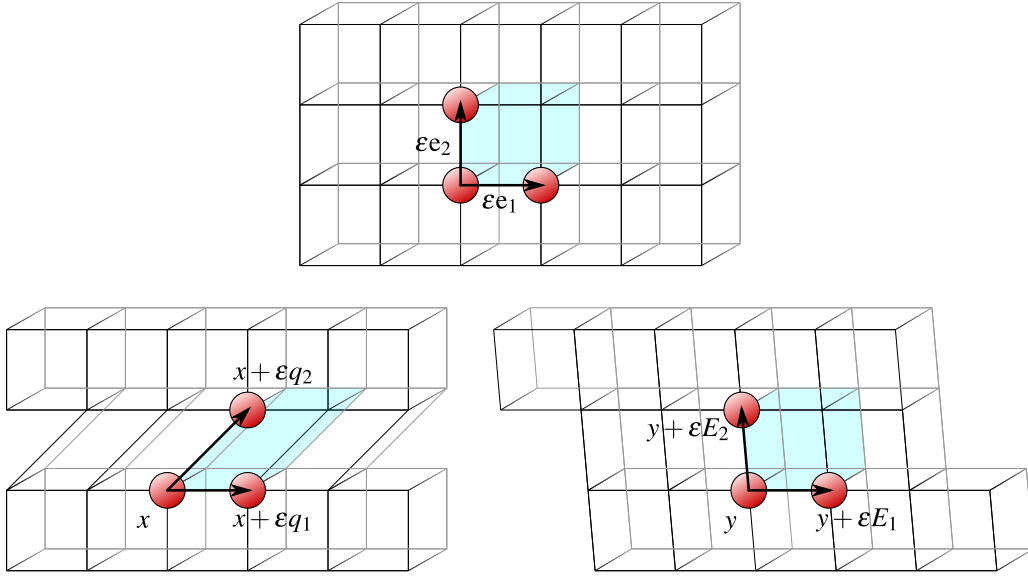


FIGURE 2. An illustration of scaffold vectors in a cubic lattice: The configuration corresponding to the bonds in the perfect lattice is shown at the top. The configuration after slip has occurred is shown on the lower left, where the atoms are held in place in their referential position and the scaffold vectors q_i show the reconnected bonds. The further elastically deformed configuration is on the lower right.

$y + \varepsilon E_i$ was previously at the position $x + \varepsilon q_i$ in the reference configuration. Since material cannot be infinitely stretched or compressed, we require that the $\{E_i\}_i$ and the $\{q_i\}_i$ are bases with the same orientation as $\{e_i\}_i$, although these bases need not be orthogonal. Under the action of the deformation gradient, the vectors q_i transform into the vectors E_i (at least to leading order as the lattice scale ε vanishes). Thus, we may equate

$$\nabla_y(x)q_i = E_i.$$

We call the vectors q_i the **scaffold vectors** of the crystal since they describe the bonds between the atoms after slip (relative to the positions of the atoms in the reference configuration). We refer to Figure 2 for an illustration.

The vectors q_i vary in time and with the referential point x to which they are attached, and we collect them as the columns of the **crystal scaffold tensor (matrix)** $Q = Q(t, x) \in \text{GL}^+(3)$. Similarly, we collect the vectors E_i as the columns of the **elastic distortion tensor (matrix)** $E \in \text{GL}^+(3)$. In this way,

$$E = \nabla_y Q.$$

We note that the construction is independent of the nature of the underlying lattice: for lattices other than the simple cubic ones, the vectors q_i instead give the transformation of axes describing the unit cell.

It would be natural to assume that q_i are (possibly rotated) lattice vectors, so that Q leaves the lattice invariant (forcing Q to lie in the lattice point group). However, since we model our material as a continuum, we relax this assumption to allow more general scaffold matrices $Q \in \text{GL}^+(3)$, assuming that the variation in the scaffold occurs smoothly on a length-scale below that of our continuum model. We discuss further restrictions on Q in Section 2.5 below.

Next, consider a mesoscopic (referential) piece $x + [0, \delta]^3$ of our specimen, where by “mesoscopic” we mean that $\delta > 0$ is small enough that the crystal scaffold vectors q_i can be considered constant in x , but large enough that any defects in the lattice can be neglected. If this piece is

cut out of the specimen, then the distorted lattice will seek to relax into its preferred shape, i.e. towards the perfect lattice. This means that the crystal scaffold vector q_i will be mapped back to e_i , and thus, the piece will attain the shape $y + P([0, \delta]^3)$, where

$$P := Q^{-1}$$

is the **plastic distortion tensor (matrix)**. While Q describes the local bond structure between points in the reference configuration, P describes how the points in the reference configuration may be locally embedded in the perfect lattice structure of the material. As $\nabla y Q = E$, this is equivalent to the multiplicative **Kröner decomposition**

$$\nabla y = EP,$$

which is often considered as fundamental to all geometrically nonlinear modeling in finite-strain elasto-plasticity [20, 43, 45, 59, 68, 69, 92].

Note that in the argument above we have implicitly assumed that the crystal wants to restore the unit cell to its original shape, which is equivalent to the requirement that the (local) elastic energy density has a minimum only at the identity matrix Id . If on the other hand this minimum should move to αId (for example through thermal expansion), then the local piece $x + [0, \delta]^3$ would instead take the shape $y + \tilde{P}([0, \delta]^3)$, where $\tilde{P} := \alpha Q^{-1}$. Moreover, if the identity matrix Id is a minimum of the energy density, then the whole point group \mathfrak{G} of the crystal will also be of minimal energy, and $PQ \in \mathfrak{G}$ would also be an admissible relation. In contrast, Q is a purely kinematic variable and makes no reference to an energy density, so may be considered more natural. In the following we will, however, avoid these ambiguities by *defining* the plastic distortion tensor as $P := Q^{-1}$.

Moving back to the macroscopic point of view, in general

$$\text{curl } P \neq 0,$$

and indeed, this is a necessary property for the modeling of dislocations as topological lattice defects. Consequently, there may be no deformation y^p with $\nabla y^p = P$, hence we only speak of E and P as the elastic and plastic “distortions”, respectively (this terminology is taken from [45]).

Note that without knowledge of the history of slip the plastically distorted shape of the crystal (i.e., P or Q) is unobservable. The model developed here will therefore be based on an explicit flow for the crystal scaffold Q , or, equivalently, the plastic distortion P . Therefore, the “uniqueness problem” for P (or Q), that is, the question which invariances should be required of E, P in order to make the Kröner decomposition unique, which is much discussed in the literature [20, 27, 43, 72, 77, 79, 85, 86, 94, 109], is not relevant here.

2.4. Burgers vectors. On a more formal mathematical level, the crystal scaffold Q maps between two different types of vectors: *structural vectors* and *displacement vectors*. Let a vector s be in “canonical lattice coordinates”, that is, *assuming the crystal is perfect and uniform*, the vector s represents a translation of s^i units in the i ’th direction relative to some standard description of a particular crystal structure. As an example, in a cubic material, such a standard description might align the coordinate directions with the edges of a cubic cell. We term such vectors s as **structural vectors**, which lie in the **local structural space** $S_x \Omega$ attached at x . Together, the structural spaces attached at all $x \in \Omega$ form the **(total) structural space** $S\Omega := \bigcup_{x \in \Omega} S_x \Omega$ (which has the mathematical structure of a vector bundle). Choosing to observe particular properties and symmetries of the structural vectors forms a modeling input into the choice of this space, since it reflects our belief about the ground-state lattice structure of the material.

On the other hand, points in the reference and deformed configurations are not taken from this perfect lattice, and are connected by **displacement vectors** in the ambient space within which the crystal sits. The spaces of displacement vectors are the tangent spaces $T_x \Omega$ (in the reference configuration) and $T_{y(x)} y(t, \Omega)$ (in the deformed configuration). We can use the matrix field Q to map structural into referential displacement vectors and the matrix field P for the reverse map. Likewise, $E = \nabla y Q$ maps structural vectors into spatial displacement vectors.

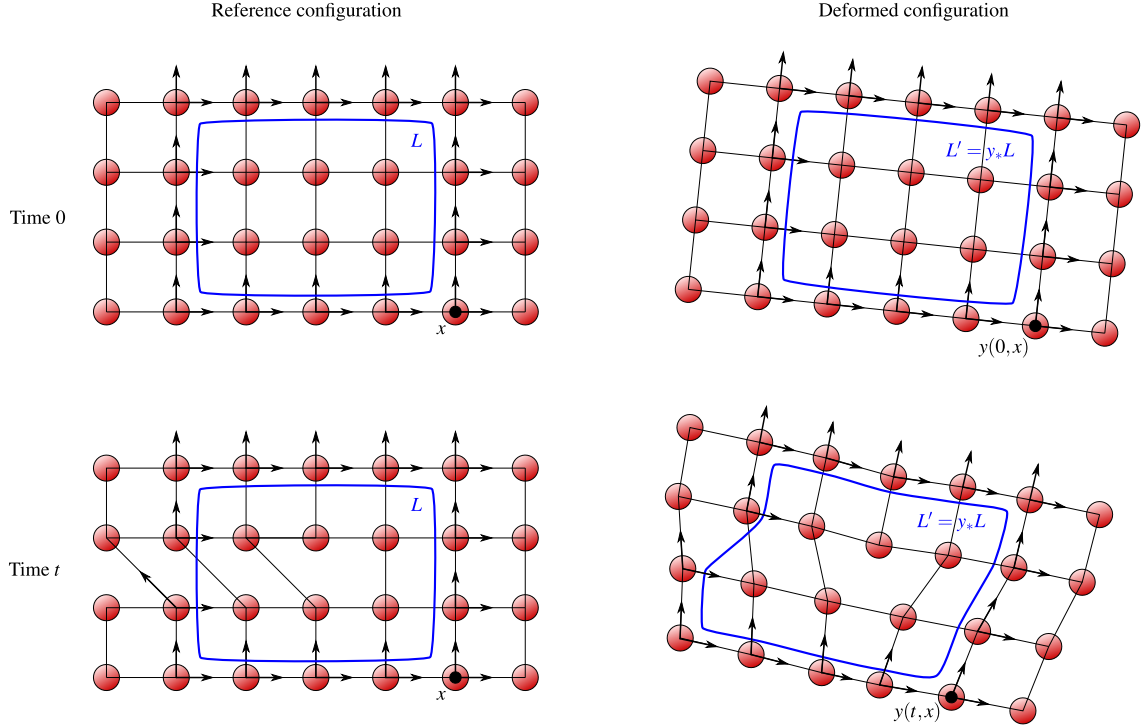


FIGURE 3. An illustration of loops around a dislocation used to find the Burgers vector.

Since the fields Q and E provide local spatial embeddings of the perfect lattice structure, we can detect certain topological defects in the structure of the lattice by considering their behavior. In this context, defects are present when tracking structural vectors $s \in \mathbb{Z}^3$ over mesoscopic distances leads to non-unique referential or spatial offsets due to *path-dependence*. Any discrepancy encountered is a **Burgers vector** as first introduced in dislocation theory [16, 17].

To illustrate this idea further and make it more precise, consider Figure 3, which illustrates a dislocation lying in a plane within a simple cubic crystal. Choose two directions e_1 and e_2 in the referential configuration. At a referential point x and time t , these map to lattice directions expressed by the structural vectors

$$p_1(t, x) := P(t, x)e_1, \quad p_2(t, x) := P(t, x)e_2.$$

Next, consider two paths in the reference configuration, starting at x . The first, ℓ_1 , involves traveling first s^1 units in the e_1 -direction and then s^2 units in the e_2 -direction. The second, ℓ_2 , involves traveling first s^2 units in the e_2 -direction and then s^1 units in the e_1 -direction. If τ is the unit tangent vector to these curves, then by integrating the structural vector density $P(t, x)\tau$ along each curve, we obtain a net structural vector which describes the total lattice displacement we experience relative to traveling through a perfect lattice. We define the discrepancy between the two results to be the Burgers vector around the referential loop $L := \ell_1 - \ell_2$:

$$\text{Burgers vector around a referential loop } L = \int_L P \cdot ds = \int_{\ell_1} P \cdot ds - \int_{\ell_2} P \cdot ds.$$

If S is the surface with normal e_3 enclosed by L , then, applying Stoke's theorem, we have that

$$\int_L P \cdot ds = \int_S \text{curl} P \cdot da,$$

where $\text{curl} = \nabla \times$ is taken row-wise. Letting the size of the loop tend to zero, we see that the Burgers vector density at (t, x) over an infinitesimal surface with normal e_3 is $\text{curl} P(t, x)e_3$. A more general construction shows that the Burgers vector density at (t, x) over an infinitesimal

surface with normal N is $\text{curl} P(t, x)N$. This corresponds precisely to Kröner's dislocation density tensor α [59–61].

In the deformed configuration, we claim that the Burgers vector can be computed in a similar way, but using $E^{-1} = P(\nabla y)^{-1}$ in place of P . Since $y(t, \cdot)$ is assumed to be a diffeomorphism, denote the inverse of the deformation map $y(t, \cdot)$ as $x(t, \cdot)$. Then we assert that

$$\text{Burgers vector around a spatial loop } L' = \int_{L'} E^{-1}(t, x(t, y)) \cdot ds'.$$

We now demonstrate that this is equivalent to the referential definition above. Using the fact that y is assumed to be a diffeomorphism, we have that any loop $L' \subset y(t, \Omega)$ is of the form $L' = y(t, L)$ for some loop $L \subset \Omega$, and so

$$\begin{aligned} \int_{L'} E^{-1}(t, x(y)) \cdot ds' &= \int_L P(t, x(y)) (\nabla y)^{-1}(t, x(y)) \cdot ds' \\ &= \int_{y(t, L)} P(t, x(y)) \nabla x(t, y) \cdot ds' \\ &= \int_L P \cdot ds. \end{aligned}$$

A similar argument as before entails that the Burgers vector density over an infinitesimal surface with normal n located at the spatial point y is $\text{curl} E^{-1}(t, x(y))n$, where the curl is taken row-wise with respect to the spatial coordinates y . We note that a direct consequence of this construction is that temporal changes in the deformation gradient ∇y alone do not affect the Burgers vector, whereas changes in P (or, equivalently, Q) do.

We conclude this discussion by remarking that the Engineering literature occasionally refers to the “structural (intermediate) configuration” between plastic and elastic distortions. This, however, can only be understood in the sense of *vectors* and then only for locally perfect and uniform lattices, as explained above. It is meaningless to talk about “structural points” since the crystal scaffold Q need not correspond to the gradient of an invertible map. Further, there is some disagreement in the literature over what should be called the “undistorted” crystal lattice, see for example [45, Section 91.2] and [85]. The *observed* lattice (which can be visualized for example through orientation-imaging microscopy) is the one that emerges after the new bonds have been formed and the atoms have relaxed their positions to an energetically optimal position. We here understand structural vectors relative to a locally perfect and uniform lattice, and so, the *undistorted* lattice resides in the “structural space” (in agreement with [45, Section 91.2]).

2.5. Incompressibility and restrictions. We motivated the introduction of the scaffold tensor (matrix) Q in Section 2.3 as a transformation which leaves the lattice invariant, but subsequently relaxed this in our continuum setting to allow for $Q \in \text{GL}^+(3)$. Here, we demonstrate that by considering the lattice-based origins of Q , we can nevertheless deduce various restrictions we should require of this field.

If $\det Q \neq 1$ at some point in the crystal, then (in an averaged sense) the unit cell has grown ($\det Q > 1$) or shrunk ($\det Q < 1$) during slip. Physically, such motion requires dislocation climb to occur, which adds or removes a plane of lattice atoms. This in turn requires interaction between dislocations and point defects [55, Chapter 3] which, as with surface defects, we neglect in our present model. Thus, in our formulation, we postulate that **plastic incompressibility** holds, i.e.

$$\det Q = 1.$$

In order to express further modeling restrictions, the plastic distortion P or, equivalently, the crystal scaffold Q , may be restricted to a real matrix Lie group

$$\mathfrak{P} \subset \text{SL}(3) := \{ Q \in \mathbb{R}^{3 \times 3} : \det Q = 1 \},$$

that is, a topologically closed group of matrices (under matrix multiplication). We call \mathfrak{P} the **plastic distortion group**; see [75, 78, 79] for earlier manifestations of this idea. So, we will

require that

$$Q \in \mathfrak{P}.$$

If no further modeling restrictions beyond the incompressibility assumption are imposed, then $\mathfrak{P} = \text{SL}(3)$, corresponding to the plastic incompressibility above.

We denote the Lie algebra associated with the Lie group \mathfrak{P} by $\mathfrak{p} = \text{Lie}(\mathfrak{P})$. It is defined to contain all those matrices $A \in \mathbb{R}^{3 \times 3}$ such that $\text{Exp}(tA) \in \mathfrak{P}$ for all $t \in \mathbb{R}$, where ‘‘Exp’’ is the matrix exponential. More abstractly, $\text{Lie}(\mathfrak{P})$ can equivalently be defined as the tangent space to \mathfrak{P} at the identity matrix, $\mathfrak{p} = T_I \mathfrak{P}$. Intuitively, an element of \mathfrak{p} represents an ‘‘infinitesimal’’ plastic distortion, or, more precisely, a **plastic rate**, i.e. the speed by which a plastic distortion changes.

Example 2.1. The following are examples of physically-relevant Lie groups \mathfrak{P} and their corresponding Lie algebras \mathfrak{p} :

- A single slip system with a unique slip direction $s \in \mathbb{R}^3$, $|s| = 1$, and slip plane normal $n \in \mathbb{R}^3$, $|n| = 1$ such that $s \perp n$, can be modeled using $\mathfrak{P} = \{ \text{Id} + \alpha(s \otimes n) : \alpha \in \mathbb{R} \}$ and its Lie algebra $\mathfrak{p} = \{ \alpha(s \otimes n) : \alpha \in \mathbb{R} \}$. This corresponds to the case where only one class of straight dislocations is permitted (the case considered in many dimension-reduced dislocation models, e.g., [19, 31, 40, 41, 84, 102, 107]).
- In many materials which have a hexagonal close-packed structure, slip occurs only on planes with normal $n = (0, 0, 1)$, but in 6 different slip directions, which may be taken to be $(\pm 1, 0, 0)$, $(\pm \frac{1}{2}, \pm \frac{\sqrt{3}}{2}, 0)$ and $(\mp \frac{1}{2}, \pm \frac{\sqrt{3}}{2}, 0)$. In this case, the slip directions have the same span as $(1, 0, 0)$ and $(-1, 0, 0)$, so we have

$$\mathfrak{P} = \{ \text{Id} + \alpha e_1 \otimes e_3 + \beta e_2 \otimes e_3 : \alpha, \beta \in \mathbb{R} \}.$$

The relevant Lie algebra is $\mathfrak{p} = \{ \alpha e_1 \otimes e_3 + \beta e_2 \otimes e_3 : \alpha, \beta \in \mathbb{R} \}$.

- In the common high-symmetry cases of face-centred cubic (FCC) and body-centred cubic (BCC) materials, where dislocation glide is the only form of motion permitted, there are sufficiently many slip directions and normals to ensure that the appropriate Lie group is the maximal one, $\mathfrak{P} = \text{SL}(3) = \{ A \in \mathbb{R}^{3 \times 3} : \det A = 1 \}$, which has the Lie algebra consisting of all deviatoric matrices, $\mathfrak{p} = \mathfrak{sl}(3) = \{ A \in \mathbb{R}^{3 \times 3} : \text{tr} A = 0 \}$.

2.6. Dislocations. As we have stated above, dislocations are line defects in the crystal lattice, which propagate slip through their motion. Their presence is characterized by a non-zero Burgers vector, which was discussed in Section 2.4 in the context of the plastic distortion. For a given material and physical regime, only a few possibilities for the Burgers vector of a dislocation are observed experimentally [9, 55]. To model this, we assume that there is a set of non-zero (structural) **Burgers vectors**

$$\mathcal{B} = \{ \pm b_1, \dots, \pm b_m \} \subset \mathbb{R}^3 \setminus \{0\}.$$

Since structural vectors reflect the lattice structure of the material, the set \mathcal{B} should be assumed to be invariant under any point symmetries of the crystal (although this requirement is not important for the derivation to follow).

In the following we will often use the convenient notation

$$\int F(b) \, d\kappa(b) := \frac{1}{2} \sum_{b \in \mathcal{B}} F(b)$$

for any function F defined on \mathcal{B} . One may interpret κ as the (purely atomic) **Burgers measure** $\kappa \in \mathcal{M}^+(\mathbb{S}^2)$ given as

$$\kappa := \frac{1}{2} \sum_{b \in \mathcal{B}} \delta_b.$$

A (referential) **dislocation system** is a collection

$$\Phi = (T^b)_{b \in \mathcal{B}},$$

where every T^b is the set of dislocations with Burgers vector b (which is constant along every slip trajectory, so both in space and time [9, 55]). So, T^b consists of oriented curves in the reference configuration Ω . Throughout this work, we will denote the consistently-oriented unit tangent vector to the collection of curves in T^b as \vec{T}^b . More precisely, every T^b can be expressed as a 1-dimensional integral current in Ω ; see Section A.2 for some elements of the theory of currents and Section A.3 for the rigorous definition of dislocation systems.

As observed physically, we assume that the curves in T^b are either closed loops or end at the boundary of the crystal, and switch orientation when the sign of the Burgers vector is switched. This can be expressed in symbols as

$$\partial T^b = 0 \llcorner \Omega, \quad T^{-b} = -T^b \quad (2.1)$$

for all $b \in \mathcal{B}$. Here, ∂T^b is the boundary operator of T^b , which is the formal sum of the point masses at the end points of the curves in T^b with their sign induced by the orientation of the respective curve (+1 at the “end” and -1 at the “start”). The symmetry condition entails that every dislocation occurs exactly twice in Φ , and hence we introduce a factor of $\frac{1}{2}$ in the definition of κ to cancel this double counting when integrating over κ . We could also consider dislocation systems which are not discrete, but we will not do so in this work.

If we want to transform to the deformed configuration, we need to consider the pushforward under the deformation, i.e., $y(t, T^b)$. Since we assume $y(t, \cdot)$ is a diffeomorphism, it is easy to verify that $y(t, T^b)$ is boundaryless inside $y(t, \Omega)$, and so dislocations remain closed loops (inside $y(t, \Omega)$) in the deformed configuration.

We note that the character of the discrete dislocation loop T^b with Burgers vector b at a referential point x is described by the relationship between \vec{T}^b and b , but in our framework these vectors are of different type: b is a structural vector but \vec{T}^b is a referential displacement vector. The correct way to compare them is therefore to map \vec{T}^b into the structural space via P , giving the curve tangent relative to the lattice. This leads us to say that if at a point x the vectors $P\vec{T}^b$ and b are orthogonal, then T^b is an *edge dislocation* at this point; if $P\vec{T}^b$ and b are parallel then T^b is an *screw dislocation*; otherwise the dislocation is of *mixed type* [55]. Note in particular that the movement of other ambient dislocations may change the type of a fixed dislocation loop since this movement changes P ; see Figure 4.

Let us also remark that some works in the literature instead consider tensor-valued currents, see, e.g., [101]. While this approach elegantly represents the symmetry $T^{-b} = -T^b$, it creates the issue that there is no uniqueness of decomposition into tensor products (at least in the case of *fields* of dislocation lines, which we do not consider in the present work). Since our expression for the dissipation will also be allowed to depend on the Burgers vector b (see Section 4 below), we choose the above b -indexed representation of dislocation systems instead.

2.7. Thickened dislocation. When considering discrete dislocations as we do here, we are dealing with the case where the individual dislocations are “macroscopically visible”. Thus, to accurately reflect their effect on the plastic distortion, we need to assign them a finite size. We do this by introducing a **dislocation line profile** $\eta: \mathbb{R}^3 \rightarrow [0, \infty)$ with compact support and satisfying $\int \eta \, dx = 1$. While a dependence of η on b or even on the tangent \vec{T}^b to the line (allowing for different shapes of edge and screw dislocations) is conceivable, for simplicity, we consider η to be fixed globally. Let “ $*$ ” denote convolution in the spatial variables. Then, the **thickened dislocation system** is defined as $\Phi_\eta := (T_\eta^b)_b$ with

$$T_\eta^b := \eta * T^b,$$

that is, T_η^b is “smeared out” with shape η (in space). The approach of assigning dislocations a finite size in order to make proper sense of their evolution within continuum models is common; see for example [18, 25].

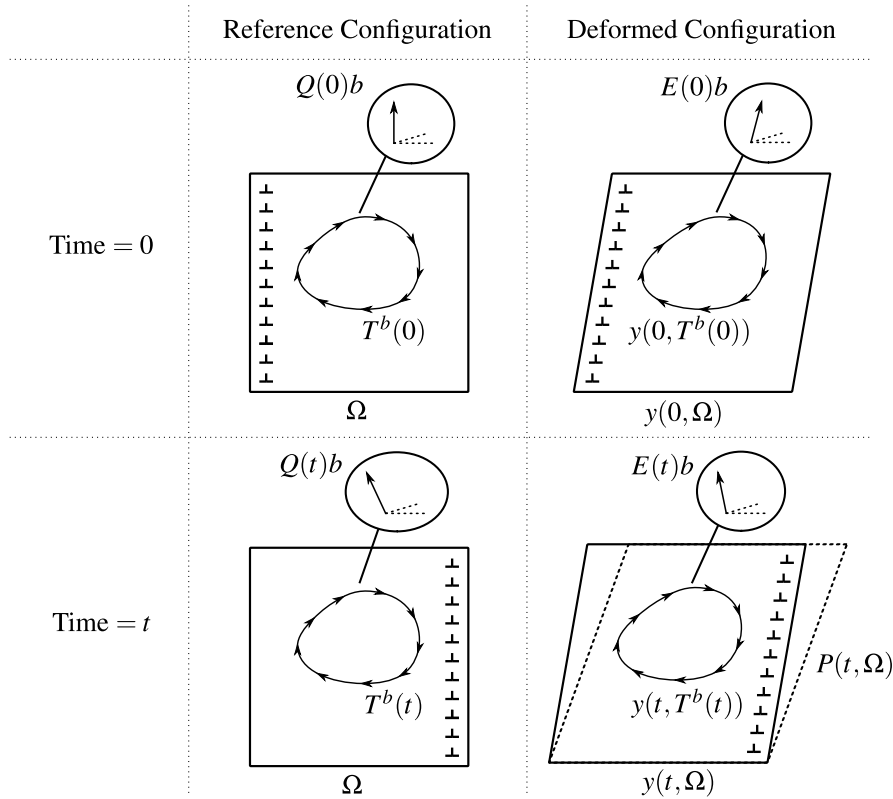


FIGURE 4. An illustration of the change to a dislocation loop under the movement of ambient edge dislocations.

3. DYNAMICS

Now that we have established a description of the kinematic quantities, we next present our approach to a dynamical theory.

3.1. Slip trajectories and velocity. In order to make clear mathematical sense of dislocation movement within our framework, we will consider the evolution of the loops T^b in (Galilean) space-time $\mathbb{R}^{1+3} \cong \mathbb{R} \times \mathbb{R}^3$, where the first component takes the role of “time” and the remaining components take the role of “space”. The unit vectors in \mathbb{R}^{1+3} are denoted by e_0, e_1, e_2, e_3 with e_0 the “time” unit vector (pointing in positive direction). We also define orthogonal projections onto the time and space components as

$$\mathbf{t}(t, x_1, x_2, x_3) := t \quad \text{and} \quad \mathbf{p}(t, x_1, x_2, x_3) := (x_1, x_2, x_3),$$

respectively. On occasion, we will consider spatial vectors in \mathbb{R}^3 as space-time vectors in \mathbb{R}^{1+3} by extending them by zero in the e_0 direction, i.e., identifying

$$(x_1, x_2, x_3) \in \mathbb{R}^3 \quad \text{with} \quad (0, x_1, x_2, x_3) \in \mathbb{R}^{1+3}.$$

A referential **slip trajectory system** over the time interval $[0, T]$ is a collection

$$\Sigma = (S^b)_{b \in \mathcal{B}},$$

where each S^b is a set of 2-dimensional oriented surfaces lying in the 4-dimensional space-time cylinder $[0, T] \times \Omega$. In this way, S^b collects the trajectories of all dislocations with Burgers vector b . A precise mathematical formulation models the S^b as 2-dimensional integral currents in space-time, which enables one to put the following derivation on a rigorous footing; see Appendix A for further details. An illustration of slip trajectories is given in Figure 5.

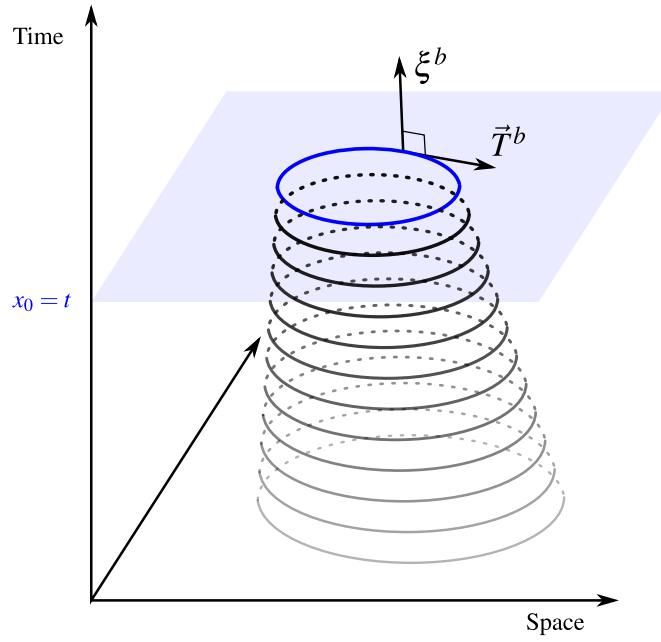


FIGURE 5. An illustration of a slip trajectory showing the evolution of a single loop in time, along with accompanying tangent vectors (for visualization purposes only two spatial dimensions are shown).

We also assume

$$S^{-b} = -S^b \quad \text{for every } b \in \mathcal{B} \quad (3.1)$$

and that S^b has no boundary on the interior of the space-time cylinder, i.e.

$$\partial S^b \llcorner ((0, T) \times \Omega) = 0, \quad (3.2)$$

where the symbol “ \llcorner ” denotes the restriction. This assumption is a natural extension of the requirement that dislocations are composed of loops inside Ω , and that these loops are not instantaneously created or destroyed, but must instead grow from or shrink to a point. As a consequence of these assumptions, for all $t \in [0, T]$, restricting S^b to the time-slice $\{t\} \times \Omega$ (and projecting onto \mathbb{R}^3) results in the dislocation system $T^b(t)$ satisfying the properties assumed in Section 2.6. More formally, one obtains $T^b(t)$ from S^b by considering the slice $S^b|_t$ (with respect to the time projection \mathbf{t}) and pushing forward under \mathbf{p} , giving the definition $T^b(t) := \mathbf{p}_*(S^b|_t)$.

Since slip trajectories are space-time surfaces, they have (two-dimensional) space-time tangent spaces. As we will see, the geometric properties of the tangent space to S^b are directly connected to properties of the dislocations whose motion they represent. Indeed, the (spatial) tangent vector $\vec{T}^b(t, x)$ to $T^b(t)$ at $x \in \Omega$, can be lifted to the (space-time) tangent space of S^b at (t, x) :

$$\vec{T}^b(t, x) \in \mathbf{T}_{(t, x)} S^b.$$

Moreover, since $|\vec{T}^b|^2 = 1$, we see that the (space-time) vector \vec{T}^b can be used as the first element of an orthonormal basis for the tangent space $\mathbf{T}_{(t, x)} S^b$. We denote the second orthonormal basis vector by $\xi^b(t, x) \in \mathbf{T}_{(t, x)} S^b$, which is uniquely defined once we require that it points “forward in time”, i.e., that

$$\mathbf{t}(\xi^b(t, x)) = \xi^b(t, x) \cdot \mathbf{e}_0 \geq 0.$$

This ξ^b we call the **geometric derivative** of the slip trajectory S^b . Hence,

$$\mathbf{T}_{(t, x)} S^b = \text{span} \{ \vec{T}^b(t, x), \xi^b(t, x) \}.$$

Physically, the above statement says that the tangent space to a slip trajectory S^b at a point (t, x) is the span of the tangent vectors to the dislocations passing through x at time t , which (by definition) have no components in the time direction, along with the geometric derivative ξ^b , which contains all information about the rate and direction of motion.

We also define the **(referential) dislocation velocity** of S^b at (t, x) as

$$\frac{D}{Dt}S^b(t, x) := v^b(t, x) := \frac{\mathbf{p}(\xi^b(t, x))}{|\mathbf{t}(\xi^b(t, x))|} \in \mathbb{R}^3.$$

To ensure that this is well-defined, we in fact require that all slip trajectories satisfy the following regularity condition:

$$\mathbf{t}(\xi^b(t, x)) = \xi^b(t, x) \cdot \mathbf{e}_0 > 0.$$

This means that the slip surface has no “vertical” parts. With $\mathbf{p}(\xi^b)$ being the spatial displacement of the dislocation (locally around a point) per $|\mathbf{t}(\xi^b)| = \xi^b \cdot \mathbf{e}_0$ units of time, the spatial velocity of the dislocation is indeed given by the above definition of $\frac{D}{Dt}S$. We further note that the dislocation velocity v^b is orthogonal to the tangent vector \vec{T}^b since, by construction, ξ^b and \vec{T}^b are orthogonal, and hence

$$0 = \xi^b \cdot \vec{T}^b = \mathbf{p}(\xi^b) \cdot \vec{T}^b = \mathbf{t}(\xi^b) v^b \cdot \vec{T}^b,$$

where we have considered \vec{T}^b both as a vector in \mathbb{R}^3 and \mathbb{R}^{1+3} . This fact expresses that the dislocation velocity does not have a component along the tangent of the curve (which would have no meaning). We further refer to Section A.4 for a more geometric view on the definition of the dislocation velocity.

3.2. Dislocation motion and infinitesimal plastic shear. As a central ingredient of our model, we now derive an expression for the change in the crystal scaffold caused by a dislocation traveling along a slip trajectory. Concretely, a dislocation with Burgers vector $b \in \mathcal{B}$ moving within a (structural) plane H' in the perfect lattice causes a rearrangement of bonds as follows: A bond s which has a component in the normal direction to H' is broken and reconnected to an adjacent lattice point $s - b$ (this choice of sign seems to be the most natural one). This action corresponds to applying a shear of the form $\text{Id} - b \otimes N'$ to each bond where N' is the (structural) normal to the plane H' . The action of this rearrangement of bonds corresponds to mapping the (referential) scaffold vector $q = Qs$ to $q - Qb$. We thus posit that the motion of a single dislocation across the plane H' yields a net transformation of scaffold vectors via

$$q \mapsto (\text{Id} - (Qb) \otimes N)q,$$

where N now is the referential normal vector corresponding to the structural normal vector N' . In this context note that $N \cdot q$ is the component of q normal to H .

If the dislocation velocity is $\frac{D}{Dt}S^b = v^b$ then the normal vector N can be expressed as

$$N = \frac{v^b \times \vec{T}^b}{|v^b \times \vec{T}^b|} = \frac{v^b \times \vec{T}^b}{|v^b|}, \quad (3.3)$$

where the second equality follows from the standard result that $|a \times b| = |a||b|$ for orthogonal vectors $a, b \in \mathbb{R}^3$. More generally, if φ^b dislocations with Burgers vector b move within the plane H , the crystal scaffold Q is transformed via the **infinitesimal plastic shear** relation

$$Q \mapsto Q' := (\text{Id} - (Qb) \otimes N \varphi^b) Q \quad \text{at time } t \text{ such that } (t, x) \in \text{supp } T^b(t). \quad (3.4)$$

We note that (3.4) implicitly assumes that lattice planes transform in a straightforward way under the scaffold map Q . This, in fact, turns out to be an issue which is slightly more subtle than it might appear at first sight. A full derivation is presented in Section A.5.

3.3. Plastic flow equation. We will now derive the plastic flow equation from the infinitesimal plastic shear relation (3.4). The arguments in this section are somewhat heuristic in order to avoid the more involved language of geometric measure theory. A more precise derivation is given in Section A.6.

Recall the definition of the thickened dislocation system $(T_\eta^b)_b$ from Section 2.7 and also define the **thickened slip trajectories** $\Sigma_\eta := (S_\eta^b)_b$ as

$$S_\eta^b := \eta * S^b.$$

Consider an infinitesimal time interval $[t, t + \delta]$ and a referential point $x \in \Omega$. Over the course of this time interval, the amount of dislocations with Burgers vector b passing through (near) this point is

$$\varphi^b(x; [t, t + \delta]) = \int_t^{t+\delta} m_\eta^b(\tau, x) |v_\eta^b(\tau, x)| \, d\tau, \quad (3.5)$$

where $m_\eta^b(s, \cdot)$ is the **multiplicity** of $T_\eta^b(s)$, that is, the (vector) norm of the density of $T_\eta^b(s)$ (with respect to Lebesgue measure), and $|v_\eta^b|$ is the speed at which the dislocations are transported past the point x . The expression in (3.6) for φ^b is equal to the value $|\mathbf{p}(S_\eta^b)|([t, t + \delta] \times \Omega)$, where we wrote the “total slip measure” as $|\mathbf{p}(S_\eta^b)| := |\mathbf{p}(\bar{S}_\eta^b)| \llcorner S_\eta^b$; this follows from the rigorous arguments made in Section A.6.

Combining the infinitesimal plastic shear relation (3.4) (for the thickened slip trajectories) with the expression for φ^b in (3.5), it follows that

$$Q(t + \delta) \approx \left(\text{Id} - (Q(t)b) \otimes N_\eta \int_t^{t+\delta} m_\eta^b(\tau) |v_\eta^b(\tau)| \, d\tau \right) Q(t). \quad (3.6)$$

Rearranging,

$$-Q(t)^{-1} \frac{Q(t + \delta) - Q(t)}{\delta} Q(t)^{-1} \approx b \otimes \frac{N_\eta}{\delta} \int_t^{t+\delta} m_\eta^b(\tau) |v_\eta^b(\tau)| \, d\tau,$$

so we may take the limit as $\delta \rightarrow 0$ to arrive at

$$-Q^{-1} \dot{Q} Q^{-1} = b \otimes g^b, \quad (3.7)$$

where we defined the **geometric slip rate** to be

$$g^b := N_\eta m_\eta^b |v_\eta^b| = v_\eta^b \times \bar{T}_\eta^b m_\eta^b = \eta * [v^b \times \bar{T}^b m^b] \in \mathbb{R}^3, \quad (3.8)$$

with m^b the multiplicity of dislocations lines in T^b (which really is a singular measure with respect to Lebesgue measure) at a point. Here we also used (3.3) for the first equality. The second equality in (3.8) follows because the mollification commutes with the operation of computing the geometric slip rate (this follows from the arguments of Section A.6). Intuitively, the geometric slip rate g^b is the normal vector field to the dislocation motion, with magnitude proportional to the velocity and number of flowing dislocations.

Finally, several slip systems with different Burgers vectors b may be active at the same time. We assume that these are additive at the level of plastic flow, and thus we obtain the **plastic flow equation**

$$\dot{P} = -Q^{-1} \dot{Q} Q^{-1} = D \quad (3.9)$$

with the **total plastic drift**

$$D(t, x) := \int b \otimes g^b(t, x) \, d\kappa(b) \in \mathbb{R}^{3 \times 3}. \quad (3.10)$$

Alternatively, and this is the approach taken in Section A.6, one may first define the 2-vector-valued geometric slip rate

$$\gamma^b(t, x) := \eta * \left[\frac{D}{Dt} S^b(t, \cdot) \wedge \bar{T}^b(t) m^b \right], \quad (3.11)$$

which arises naturally as the quantity describing the flow of dislocations via the coarea formula. We note that a 2-vector $a \wedge b$ represents the oriented plane spanned by the vectors a and b , which, in 3-dimensional space (but not in 4-dimensional space-time), can equivalently be represented by its oriented normal $a \times b$. In \mathbb{R}^3 , the transformation between 2-vectors and normal vectors is given via Hodge duality, and g^b defined in (3.8) is indeed the Hodge dual of γ^b . We again refer to Section A.6 for further details.

Example 3.1. Assume just plastic incompressibility, that is, $\mathfrak{P} = \text{SL}(3)$, so $\det Q = 1$. Then, $\mathfrak{p} = \mathfrak{sl}(3)$, the vector space of deviatoric (i.e., trace-free) matrices. Using Jacobi's formula and Cramer's rule (whereby $Q^{-1} = (\text{cof } Q)^T$), we compute

$$\frac{d}{dt} \det Q = \text{cof } Q : \dot{Q} = \text{tr}(Q^{-1} \dot{Q}) = -\text{tr}(QD).$$

Thus, if the initial value Q_0 for Q satisfies $\det Q_0 = 1$ (everywhere in Ω), then for the preservation of this property, QD needs to be deviatoric,

$$\text{tr}(QD) = 0.$$

Using the formula (3.10) for D , this holds if Qb is orthogonal to g^b (the normal to the slip trajectories), which is the case precisely if the dislocation motion is a *glide* [9, 55] since Qb is the referential manifestation of the (structural) Burgers vector b . If there is dislocation *climb*, then $(Qb) \cdot g^b \neq 0$ and the plastic flow is not volume-preserving. We note that it is natural that this condition depends on Qb and not b directly: In an distorted crystal the scaffold (which is expressed in referential coordinates) has changed and so the (referential) slip planes along which the crystal can deform in a volume-preserving fashion, have changed with it; for an illustration, see Figure 4. For a brief discussion of how climb might be incorporated into the present model, we refer to Section 6.2.

3.4. Consistency. In our model, there are two different ways of detecting dislocations in the specimen: First, the dislocations are given explicitly in the dislocation system $(T^b(t))_b$ at time t . Second, they can be detected by computing the circulation of P around the dislocation and adding up tangent (lattice) vectors, as explained in Section 2.4. This is equivalent to P having a non-trivial curl, i.e.

$$\text{curl } P \neq 0.$$

For the consistency of our model it is important to verify that the defects expressed in $P(t)$ remain the same as the ones expressed in the dislocation system $(T^b(t))_b$. Indeed, the dynamics preserve the **consistency condition**

$$\text{curl } P(t) = \int b \otimes T_\eta^b(t) \, d\kappa(b) \quad \text{in } \Omega \quad (3.12)$$

along the flow. This means that (3.12) holds for all $t \in (0, T)$ if it is satisfied at $t = 0$, where we assume it as a condition on the initial data. A full proof of (3.12) requires the use of geometric tools, and so the details are postponed to Section A.7.

4. ENERGETICS

We next apply two fundamental principles of energetic modeling in mechanics. First, for the *Principle of Virtual Power* [45, Chapter 92] one considers all “virtual” motions of the system under consideration, that is, all allowed motions within the independent degrees of freedom. These motions are referred to as “virtual” because they might not be attained in a given evolution (but they are *attainable*). Concretely, the motions our system can undergo are the variations in the total deformation y of the specimen and movement of the dislocations via a slip trajectory Σ . The other quantities P (or Q) and E only change as a consequence of movement in y and the slip trajectory Σ . Second, we will invoke the *Free Energy Imbalance* [45, Section 27.3], which is a version of the *Second Law of Thermodynamics*, to obtain a relation on the directionality of the evolution.

4.1. **Energy and stresses.** For a deformation y , which is an orientation-preserving diffeomorphism and hence satisfies $\det \nabla y > 0$, and a scaffold map Q , we define the **elastic energy** via

$$\mathcal{W}_e(y, Q) := \int_{\Omega} W_e(\nabla y Q) \, dx, \quad (4.1)$$

where $W_e: \text{GL}^+(3) \rightarrow \mathbb{R}$ is the **elastic energy density**. This shape of the energy functional is explained as follows: Postulating the Cauchy–Born rule [32, 33, 36, 51, 89], the elastic potential energy of the deformation will depend on $E = \nabla y Q$ only, since E encodes the stretching of the bonds in a crystal unit cell.

We further require W_e to satisfy the **objectivity (frame-indifference)** condition

$$W_e(RE) = W_e(E) \quad \text{for all } R \in \text{SO}(3), E \in \text{GL}^+(3). \quad (4.2)$$

Often, W_e also reflects additional material symmetries, such as $W_e(EZ) = W_e(E)$ for all Z from a **(point) symmetry group** $\mathfrak{G} \subset \text{SL}(3)$ of the crystal. A common material symmetry is **isotropy**, for which $\mathfrak{G} = \text{SO}(3)$, see, e.g., [21, Section 3.4] and [42]. Note that for $Z \in \mathfrak{G}$ we have $EZ = \nabla y QZ$ and the corresponding scaffold $Q' := QZ$ represents a symmetry transformation of the lattice.

Let $f(t) = f(t, x) \in \mathbb{R}^3$ be an external **bulk loading**; here, we avoid explicitly considering other types of loading to minimize complexity, but there is of course no significant restriction on the form this can take. We then define the **total energy** as

$$\mathcal{E}(t, y, Q) := \mathcal{W}_e(y, Q) - \int f(t) \cdot y \, dx. \quad (4.3)$$

Let $\Omega' \subset \Omega$ be a referential subdomain of the body Ω . The **internal power** expended within Ω' is given as

$$\mathcal{I}(\Omega') = \int_{\Omega'} \frac{d}{dt} W_e(\nabla y Q) \, dx + \int \int_{\Omega'} X^b \cdot g^b \, dx \, d\kappa(b)$$

where $X^b \in \mathbb{R}^3$ ($b \in \mathcal{B}$) is the **referential configurational stress** that is power-conjugate to the geometric slip rate g^b . Section 4.6 below will show how X^b can be considered a nonlinear analogue of the Peach–Koehler force [90].

Assuming that we may differentiate freely, we compute

$$\dot{E} = \nabla \dot{y} Q + \nabla y \dot{Q} = \nabla \dot{y} Q + \nabla y Q L = \nabla \dot{y} Q + E L,$$

where

$$L := \dot{P} P^{-1} = Q^{-1} \dot{Q}.$$

is the **structural plastic rate**. Then,

$$\begin{aligned} \frac{d}{dt} W_e(\nabla y Q) &= D W_e(E) : \dot{E} \\ &= D W_e(\nabla y Q) Q^T : \nabla \dot{y} + Q^T \nabla y^T D W_e(\nabla y Q) : L \\ &= T : \nabla \dot{y} + M : L, \end{aligned}$$

where we have defined the **Piola–Kirchhoff stress** (referential elastic stress) as

$$T := D W_e(\nabla y Q) Q^T$$

and the **Mandel stress** (structural plastic stress) as

$$M := Q^T \nabla y^T D W_e(\nabla y Q) = E^T D W_e(E). \quad (4.4)$$

We observe that the structural plastic drift L can be related, via the plastic flow equation (3.9), to the referential plastic drift given in (3.10) as follows:

$$L = Q^{-1} \dot{Q} Q^{-1} Q = -D Q = - \left(\int b \otimes g^b \, d\kappa(b) \right) Q,$$

and thus

$$\begin{aligned} \int_{\Omega'} M : L \, dx &= - \int \int_{\Omega'} [MQ^T] : [b \otimes g^b] \, dx \, d\kappa(b) \\ &= - \int \int_{\Omega'} (QM^T b) \cdot g^b \, dx \, d\kappa(b). \end{aligned}$$

Combining the above considerations and also using the Gauss–Green theorem,

$$\begin{aligned} \mathcal{I}(\Omega') &= \int_{\Omega'} T : \nabla \dot{y} + M : L \, dx + \int \int_{\Omega'} X^b \cdot g^b \, dx \, d\kappa(b) \\ &= - \int_{\Omega'} \text{Div} T \cdot \dot{y} \, dx + \int_{\partial\Omega'} Tn \cdot \dot{y} \, da - \int \int_{\Omega'} (QM^T b) \cdot g^b \, dx \, d\kappa(b) \\ &\quad + \int \int_{\Omega'} X^b \cdot g^b \, dx \, d\kappa(b). \end{aligned}$$

On the other hand, the **external power** expended on Ω' is given by

$$\mathcal{P}(\Omega') = \int_{\partial\Omega'} t(n) \cdot \dot{y} \, da + \int_{\Omega'} f \cdot \dot{y} \, dx - \int_{\Omega'} \rho \ddot{y} \cdot \dot{y} \, dx,$$

where $t(n) \in \mathbb{R}^3$ is the surface traction in the direction of the exterior normal n and $\rho > 0$ is the mass density.

4.2. Force balance. We now postulate, as in the general theory of continuum mechanics, the fundamental *Principle of Virtual Power* [45, Chapter 92]:

The internal and external powers are equal, $\mathcal{I}(\Omega') = \mathcal{P}(\Omega')$, for all allowed motions and all $\Omega' \subset \Omega$.

Since \dot{y} and g^b are independent degrees of freedom, this yields

$$\int_{\partial\Omega'} (Tn - t(n)) \cdot \dot{y} \, da + \int_{\Omega'} (\rho \ddot{y} - \text{Div} T - f) \cdot \dot{y} \, dx = 0$$

and

$$- \int \int_{\Omega'} (QM^T b) \cdot g^b \, dx \, d\kappa(b) + \int \int_{\Omega'} X^b \cdot g^b \, dx \, d\kappa(b) = 0.$$

Then, since $\Omega' \subset \Omega$ was arbitrary, we obtain (we drop the boundary equation since we do not discuss boundary conditions in the following)

$$(\rho \ddot{y} - \text{Div} T) \cdot \dot{y} = f \cdot \dot{y} \quad \text{in } \Omega,$$

and

$$\int X^b \cdot g^b \, d\kappa(b) = \int (QM^T b) \cdot g^b \, d\kappa(b) \quad \text{in } \Omega.$$

As the virtual rates \dot{y} and g^b can attain any value, we conclude the **elastic force balance**

$$\rho \ddot{y} - \text{Div}[DW_e(\nabla y)Q^T] = f \quad \text{in } \Omega, \quad (4.5)$$

as well as the (referential) **plastic force balance** (for all $b \in \mathcal{B}$)

$$X^b = QM^T b = Q(DW_e(\nabla y)Q)^T \nabla y Q b = Q(DW_e(E))^T E b \quad \text{in } \Omega. \quad (4.6)$$

We note that we could alternatively have expressed the plastic force balance in the structural configuration, writing

$$PX^b = Q^{-1}X^b = M^T b = (DW_e(\nabla y)Q)^T \nabla y Q b = (DW_e(E))^T E b,$$

which pairs the structural configurational stress PX^b with the structural rate $Q^T g^b$. Indeed, the constitutive assumptions we discuss in the following section will indeed relate the structural stress PX^b to the structural rate $Q^T g^b$. We remark that while the stress depends upon the frame in which we express it, the power does not.

We further impose the *Free Energy Imbalance* [45, Section 27.3], which is itself a consequence of the *Second Law of Thermodynamics*:

Along the evolution it holds that $\frac{d}{dt}\mathcal{W}_e(\Omega') - \mathcal{P}(\Omega') = -\Delta(\Omega') \leq 0$ in every subregion $\Omega' \subset \Omega$.

By the *Principle of Virtual Power* we also have $\mathcal{P}(\Omega') = \mathcal{I}(\Omega')$. Thus we obtain

$$\frac{d}{dt}\mathcal{W}_e(\Omega') - \mathcal{I}(\Omega') = -\Delta(\Omega') \leq 0.$$

Using analogous derivations like the ones for the internal power above, we obtain the **dissipation relation**

$$\int \int_{\Omega'} X^b \cdot g^b \, dx \, d\kappa(b) = \Delta(\Omega') \geq 0, \quad (4.7)$$

where $\Delta(\Omega') \in [0, +\infty)$ is the **dissipation rate** in Ω' . This expresses the *irreversibility* of plastic flow whenever $\Delta(\Omega') > 0$. In contrast, purely elastic deformations (for which $g^b \equiv 0$) are reversible.

4.3. Flow rule. So far we have not constitutively specified the configurational stresses X^b in (4.6). We propose that (4.6) can be written as a differential inclusion for a function of the *structural* rate $Q^T g^b$, where g^b is the geometric rate. This expresses the idea that rates must be mapped into the lattice in order to evaluate the energy dissipated, or, in other words, stresses depend only on the structural rates. Indeed, since in our model the primary source of anisotropy lies in the crystal lattice (different behavior along the crystal vectors), the structural dissipation potentials have a good chance of being “simpler” than their referential counterparts. This approach is in agreement with the formulation for phenomenological plastic evolution in much of the literature (see, e.g., [45, 79]).

So, we assume the following (see also [39, Section 4.4] and [103] for similar models):

There are **dissipation (pseudo)potentials** $R^b: \mathbb{R}^3 \rightarrow [0, +\infty)$ ($b \in \mathcal{B}$), which are proper ($\neq +\infty$), convex, lower semicontinuous, and satisfy $R^b(0) = 0$ as well as the symmetry relation $R^{-b}(-\xi) = R^b(\xi)$ for all $b \in \mathcal{B}$, such that the **flow rule (Biot inclusion)**

$$PX^b \in \partial R^b(Q^T g^b) \quad (4.8)$$

holds.

Here, “ ∂R^b ” denotes the convex subdifferential of R^b , that is, $\partial R^b(Q^T g^b)$ consists of all those (**normal**) **flow stresses** $\sigma \in \mathbb{R}^3$ that satisfy

$$R^b(Q^T g^b) + \sigma \cdot (\xi - Q^T g^b) \leq R^b(\xi) \quad \text{for all } \xi \in \mathbb{R}^3.$$

Note that PX^b is the structural configurational stress, which is power-conjugate to the (structural) geometric slip rate $Q^T g^b$, so (4.8) indeed pairs power-conjugate quantities. That the flow rule is formulated as a *differential inclusion* is chiefly a constitutive assumption, cf. Section 4.4 in [39] as well as [79, 103, 110]. In principle, we can also allow for more general dissipation (pseudo)potentials, with R^b depending on further quantities, such as the type of dislocation (edge or screw). For notational reasons we have not written such dependencies explicitly.

If R^b is positively k -homogeneous ($k \geq 0$), then the convexity of R^b expresses the following intuitive constraint: When the system is moving in direction $\xi = (1 - \theta)\xi_0 + \theta\xi_1 \neq 0$, where $\xi_0, \xi_1 \in \mathbb{R}^3 \setminus \{0\}$, $\theta \in (0, 1)$, then the frictional power is $\xi \cdot \partial R(\xi) = kR(\xi)$ (element-wise, by Euler’s positive homogeneity theorem). Alternatively, the rate could oscillate very quickly between rates ξ_0, ξ_1 with time-fractions $1 - \theta$ and θ , respectively, which would result in the frictional power $(1 - \theta)kR(\xi_0) + \theta kR(\xi_1)$. The convexity tells us that this oscillatory path expends at least as much energy as the non-oscillatory one. In fact, if this is not satisfied (e.g., because of the presence of microstructure), then the material would choose the oscillatory paths in an optimal way at a small

length scale. Hence, at the meso- or macroscopic length scale we would observe the *effective* dissipation potential, which is a suitable relaxation of the microscopic dissipation potential; see [25] for a similar effect. Moreover, it can be shown that the *Maximum Plastic Work Principle*, which is a strengthening of the *Second Law of Thermodynamics*, implies convexity of R^b , see [46, pp.57–59]. The lower semicontinuity is a minimal continuity assumption and can again be justified on physical grounds (similarly to the justification of convexity).

According to the Coleman–Noll procedure [23, 44, 45], thermodynamic reasoning should give *constitutive restrictions*. In this spirit, combining (4.7) with the flow rule (4.8) yields the **strict positivity** condition on the dissipation potential R^b :

$$\xi \cdot \partial R^b(\xi) > 0 \text{ (element-wise) for non-zero } \xi \in \mathbb{R}^3.$$

Thus, energy is dissipated if and only if the material flows plastically. Whenever R^b is positively homogeneous of any order, then this is equivalent to $R^b(\xi) > 0$ for $\xi \neq 0$ (again by Euler’s positive homogeneity theorem).

If we prescribe that $P \in \mathfrak{P}$ for a Lie group $\mathfrak{P} \subset \text{SL}(3)$ as in Section 2.5, then we need to require that $QD \in \mathfrak{p}$, so that $\dot{Q}Q^{-1} \in \mathfrak{p}$ and the plastic flow does not leave \mathfrak{P} . According to the definition of the total plastic drift D in (3.10), this is true if $Qb \otimes g^b \notin \mathfrak{p}$ implies $R^b(Q^T g^b) = +\infty$. Then, $\partial R^b(Q^T g^b) = \emptyset$, and so the flow cannot progress. Setting $\xi := Q^T g^b$ and using that $Qb \otimes g^b \notin \mathfrak{p}$ if and only if $b \otimes \xi = b \otimes (Q^T g^b) \notin \mathfrak{p}$, we arrive at the following condition, which acts as a restriction on the constitutive choice of R^b :

$$\text{If } b \otimes \xi \notin \mathfrak{p} \text{ for } \xi \in \mathbb{R}^3, \text{ then } R^b(\xi) = +\infty.$$

Example 4.1. If $\mathfrak{P} = \text{SL}(3)$ then, as shown in Example 3.1, we need that $\text{tr}(QD) = 0$. To ensure this, the above condition reads as follows: If $R^b(Q^T g^b) < +\infty$, then $b \perp Q^T g^b$. In this case,

$$0 = \text{tr}(b \otimes Q^T g^b) = \text{tr}((b \otimes g^b)Q) = \text{tr}((Qb) \otimes g^b).$$

Hence, if the above condition on R^b holds, then indeed $\text{tr}(QD) = \text{tr}(DQ) = 0$ along the flow. Note that $b \perp Q^T g^b$ is equivalent to $Qb \perp g^b$, i.e., the characteristic relation for dislocation glide.

Finally, we observe that the flow rule (4.8) can also be written referentially as $X^b \in \partial \widehat{R}^b(Q, g^b)$, where the subdifferential is taken in the second variable, and $\widehat{R}^b(Q, g^b) := R^b(Q^T g^b)$. Furthermore, if we wish to formulate the problem in terms of the 2-vector-valued geometric rate γ^b (defined in Appendix A.6 as the Hodge dual of g^b) and a conjugate stress $\widetilde{X}^b \in \wedge^2 \mathbb{R}^3$, we can do so by defining an alternate dissipation potential $\widetilde{R}^b : \wedge_2 \mathbb{R}^3 \rightarrow [0, +\infty]$ via $\widetilde{R}^b(\xi) = R^b(\star \xi)$ (where \star is the Hodge star defined in Section A.1) for any $\xi \in \wedge_2 \mathbb{R}^3$. The flow rule then becomes

$$Q^T \widetilde{X}^b \in \partial \widetilde{R}^b(P\gamma^b). \quad (4.9)$$

To explain the relationship between $P\gamma^b$ and $Q^T g^b$, we recall that g^b is the oriented unit normal to the plane defined by the 2-vector γ^b , as defined in (3.11) and discussed further in Section A.6. When considering the dissipation caused by dislocation motion represented by γ^b , it is natural to transform this plane into the structural configuration using the inverse of the scaffold map, $P = Q^{-1}$, so that we consider any motion within the undistorted lattice. However, as Q need not be an orthogonal transformation, the normal vector to the resulting structural plane is not simply transformed by P . Instead, we find that if $\gamma^b \mapsto P\gamma^b$, then $g^b \mapsto P^{-T} g^b = Q^T g^b$ (and $Q^T \neq P$ if P is not orthogonal). A full argument explaining this effect is given in Section A.5.

4.4. Duality and stability. One may further define the **dual dissipation potential** $R^{b*} : \mathbb{R}^3 \rightarrow [0, +\infty]$ as the convex conjugate function of R^b , that is,

$$R^{b*}(\sigma) := \sup \{ \langle \xi, \sigma \rangle - R^b(\xi) : \xi \in \mathbb{R}^3 \}, \quad \sigma \in \mathbb{R}^3.$$

Then, by standard results in convex analysis, see for example [99], we have that R^{b*} is also proper, convex, lower semicontinuous, and satisfies the same symmetry relation as the R^b . Moreover, the

flow rule (4.8) is equivalent to the **dual flow rule (Onsager inclusion)**,

$$Q^T g^b \in \partial R^{b*}(PX^b). \quad (4.10)$$

This follows from the Legendre–Fenchel theorem and standard rules for the computation of convex conjugates.

It is a fundamental property of elasto-plastic processes that if the (structural) configurational stress PX^b lies in the interior of an **elastic stability domain** $\mathcal{S}^b \subset \mathbb{R}^3$ ($b \in \mathcal{B}$), then no plastic flow takes place. The thinking here is that below the stress threshold $\partial \mathcal{S}^b$, which is called the **yield surface**, no plastic slip can be activated. This is in very good agreement with experiments, see Chapter 5 in [70]. We set

$$\mathcal{S}^b := \partial R^b(0) \subset \mathbb{R}^3.$$

It follows from standard results in convex analysis that \mathcal{S}^b is a closed, convex neighborhood of the origin and $\mathcal{S}^{-b} = -\mathcal{S}^b$.

Define the **rate-independent dissipation potential** $R_1^b: \mathbb{R}^3 \rightarrow [0, +\infty]$ as the support function of \mathcal{S}^b , i.e., the dual of the characteristic function $\chi_{\mathcal{S}^b}$ of \mathcal{S}^b (which is 0 on \mathcal{S}^b and $+\infty$ otherwise),

$$R_1^b(\xi) := \chi_{\mathcal{S}^b}^*(\xi) = \sup_{\sigma \in \mathcal{S}^b} \langle \xi, \sigma \rangle.$$

We note that $R_1^b \geq 0$ since $0 \in \mathcal{S}^b$. Moreover, let the **residual dissipation potential** $R_+^b: \mathbb{R}^3 \rightarrow [0, +\infty]$ be defined as $R_+^b := R^b - R_1^b$, so that we have the splitting

$$R^b(\xi) = R_1^b(\xi) + R_+^b(\xi), \quad \xi \in \mathbb{R}^3.$$

It can be seen by arguing via supporting hyperplanes of the epigraph of R_+^b that R_+^b is proper, convex, lower semicontinuous, non-negative, $R_+^b(0) = 0$, and the same symmetry relation as for R^b holds.

Using the inf-convolution $(f \square g)(x) := \inf_z [f(x-z) + g(z)]$ for proper, convex, lower semicontinuous f, g , and the associated duality rule $[f \square g]^* = f^* + g^*$ (see Theorem 16.4 of [99]), we compute

$$R^{b*} = [R_1^b + R_+^b]^* = [R_1^b]^* \square R_+^{b*} = \inf_{\sigma \in \mathcal{S}^b} R_+^{b*}(\cdot - \sigma).$$

In particular,

$$R^{b*}(P\sigma^b) = 0 \quad \text{if } P\sigma^b \in \mathcal{S}^b.$$

Consequently,

$$\partial R^{b*}(P\sigma^b) = \{0\} \quad \text{if } P\sigma^b \in (\mathcal{S}^b)^\circ,$$

where $(\mathcal{S}^b)^\circ := \mathcal{S}^b \setminus \partial \mathcal{S}^b$ is the interior of \mathcal{S}^b . This expresses the idea that the flow stops once the stress attains a value in the interior the elastic stability domain \mathcal{S}^b , as required.

4.5. Dissipation. For the dissipation one can consider two main possibilities:

- (i) *The rate-dependent case:* $R_+^b(\xi) > 0$ for all $\xi \neq 0$.
- (ii) *The rate-independent case:* $R_+^b \equiv 0$.

The former case corresponds to modeling situations for which the rate of loading and of dislocation motion are comparable, while the latter corresponds to the case where dislocation motion is much more rapid than the loading rate. In this context we also refer to [50] for an example where a rate-dependent dissipation potential for dislocation motion is derived from first principles.

Example 4.2. In rate-dependent plasticity theory it is common to choose a power law for the dissipation potential $R^b: \mathbb{R}^3 \rightarrow [0, \infty)$, see for instance [45, Section 101]. For this, set for $\kappa > 0$ and $N > 1$,

$$R^b(\xi) := \frac{\kappa}{1 + 1/N} |\xi|^{1+1/N}, \quad \xi \in \mathbb{R}^3,$$

where $|\cdot|$ is a vector norm (e.g., the Euclidean norm in the isotropic case). Then, $DR^b(\xi) = \kappa|\xi|^{1/N}$ and also

$$R^{b*}(\sigma) = \frac{\kappa^{-N}}{1+N} |\sigma|_*^{1+N}, \quad \sigma \in \mathbb{R}^3,$$

with $|\cdot|_*$ the dual norm to $|\cdot|$.

We define the **(total) dissipation** over an interval $[s, t]$ as

$$\text{Diss}([s, t]) := \int_s^t \Delta(\tau) \, d\tau = \int_s^t \int_{\Omega} \int_{\Omega} X^b \cdot g^b \, dx \, d\kappa(b) \, d\tau \geq 0. \quad (4.11)$$

Now use the Legendre–Fenchel theorem to obtain the splitting

$$\begin{aligned} \text{Diss}([s, t]) &= \int_s^t \int_{\Omega} \int_{\Omega} X^b \cdot g^b \, dx \, d\kappa(b) \, d\tau \\ &= \int_s^t \int_{\Omega} \int_{\Omega} PX^b \cdot Q^T g^b \, dx \, d\kappa(b) \, d\tau \\ &= \int_s^t \int_{\Omega} \int_{\Omega} R^b(Q^T g^b) + R^{b*}(PX^b) \, dx \, d\kappa(b) \, d\tau \\ &= \int_s^t \int_{\Omega} \int_{\Omega} R_1^b(Q^T g^b) + R_+^b(Q^T g^b) + R^{b*}(PX^b) \, dx \, d\kappa(b) \, d\tau \\ &= \text{Diss}_1([s, t]) + \text{Diss}_+([s, t]) \end{aligned}$$

with

$$\text{Diss}_1([s, t]) := \int_s^t \int_{\Omega} \int_{\Omega} R_1^b(Q^T g^b) \, dx \, d\kappa(b) \, d\tau$$

and

$$\text{Diss}_+([s, t]) := \int_s^t \int_{\Omega} \int_{\Omega} R_+^b(Q^T g^b) + R^{b*}(PX^b) \, dx \, d\kappa(b) \, d\tau.$$

In the rate-dependent case, we have $PX^b \in \partial R_1^b(Q^T g^b) + DR_+^b(Q^T g^b)$. Furthermore, we use Euler's homogeneity theorem to see that $(Q^T g^b) \cdot \partial R_1^b(Q^T g^b) = R_1^b(Q^T g^b)$ (element-wise). Then, $PX^b \cdot Q^T g^b = R_1^b(Q^T g^b) + (Q^T g^b) \cdot DR_+^b(Q^T g^b)$ and so

$$\text{Diss}_+([s, t]) = \int_s^t \int_{\Omega} \int_{\Omega} (Q^T g^b) \cdot DR_+^b(Q^T g^b) \, d\kappa(b) \, d\tau.$$

In the rate-independent case, $R^{b*} = \chi_{\mathcal{S}^b} = R_1^{b*}$ so $\text{Diss}_+([s, t]) = 0$.

4.6. Linearization and Peach–Koehler force. In this final section we demonstrate that linearizing our formulation yields the classical expressions of linear elasto-plasticity.

We suppose that the total deformation gradient is expressible as a perturbation of the identity, i.e., $y(t, x) = x + u(t, x)$, where $u = u(t, x) \in \mathbb{R}^3$ is the displacement. We assume further that the displacement gradient ∇u is uniformly small, so that the deformation gradient is a perturbation of the identity matrix, $\nabla y = \text{Id} + \nabla u$. Likewise, we assume that the plastic distortion can also be expressed as a perturbation of the identity, $P(t, x) = \text{Id} + Z(t, x)$, where Z is again uniformly small (and of a comparable magnitude to the displacement gradient ∇u). The linearized form of the plastic flow equation (3.9) becomes

$$\dot{P} = \dot{Z} = D.$$

Considering the elastic strain next, we note that E can be formally expanded and approximated as

$$E = \nabla y Q = (\text{Id} + \nabla u)(\text{Id} + Z)^{-1} = \text{Id} + \nabla u - Z - \nabla u Z + Z^2 + \dots \approx \text{Id} + \nabla u - Z.$$

This leads to the usual definition of the linearized elastic distortion $\beta_e := \nabla u - Z$. Taylor-expanding the Piola–Kirchhoff stress, and assuming that the state of zero elastic strain is stress free, i.e.,

$DW_e(\text{Id}) = 0$, we define the fourth-order elastic tensor $C := D^2W_e(\text{Id})$. Then, retaining only the terms linear in β_e , we obtain that

$$T = DW_e(E)Q^T = DW_e(\text{Id} + \beta_e)(\text{Id} + Z)^{-T} \approx D^2W_e(\text{Id}) : \beta_e = C : \beta_e.$$

As a result, the linearized form of the elastic force balance (4.5) becomes

$$\rho \ddot{u} - \text{Div}[C : \beta_e] = f.$$

Applying similar considerations to the expression for the Mandel stress in (4.4), we have

$$M = E^T DW_e(E) = (\text{Id} + \beta_e)^T DW_e(\text{Id} + \beta_e) \approx (\text{Id} + \beta_e)^T C : \beta_e \approx C : \beta_e.$$

and so the linearized Mandel stress is identical to the linearized Piola–Kirchhoff stress, in contrast to the fully nonlinear setting.

Early in the development of the theory of dislocations, the force acting on a dislocation line within a linear theory of elasto-plasticity was derived through a thermodynamical argument [90]. Neglecting line tension and terms that are quadratic in β_e or Z , the configurational stress X^b can be approximated as follows:

$$X^b = QM^T b = (I + Z)^{-1} M^T b \approx (I - Z + \dots) M^T b \approx (C : \beta_e)^T b.$$

We can manipulate the pairing between the configurational stress X^b and the geometric rate g^b to approximate the rate of power expended by a moving dislocation as

$$X^b \cdot g^b \approx (C : \beta_e)^T b \cdot \left(\eta * [v^b \times \vec{T}^b m^b] \right).$$

The Peach–Koehler force [90] was formally derived as the force which acts to oppose the motion of an infinitesimally thin dislocation, so that the power expended is equated with the negative of the work done by this force,

$$X^b \cdot g^b = -f^b \cdot v^b.$$

Formally setting η to be a Dirac delta, and $m^b = 1$ to reflect the case of a single dislocation, and manipulating the expression above using the permutation invariance of the scalar triple product, we have

$$((C : \beta_e)^T b) \cdot [v^b \times \vec{T}^b] = v^b \cdot [\vec{T}^b \times ((C : \beta_e)^T b)] = -v^b \cdot [((C : \beta_e)^T b) \times \vec{T}^b],$$

and so we find through this linearization process that we obtain the classical definition of the Peach–Koehler force, namely

$$f^b = ((C : \beta_e)^T b) \times \vec{T}^b.$$

5. SUMMARY OF MODEL

In the following we summarize the relations making up our model.

- (1) Fundamental variables: $y = y(t, x) \in \mathbb{R}^3$ the deformation and $Q = Q(t, x) \in \text{SL}(3)$ the crystal scaffold, or, equivalently, $P = Q^{-1}$ the plastic distortion.
- (2) Kröner decomposition: $\nabla = EQ^{-1} = EP$, where $E := \nabla_y Q$ is the elastic distortion.
- (3) Plastic restriction: $Q \in \mathfrak{P}$ for a Lie group $\mathfrak{P} \subset \text{SL}(3)$ with Lie algebra $\mathfrak{p} = \text{Lie}(\mathfrak{P})$.
- (4) Burgers measure: $\kappa := \frac{1}{2} \sum_{b \in \mathcal{B}} \delta_b$.
- (5) Slip trajectories: A collection of two-dimensional surfaces in space-time, $\Sigma = (S^b)_{b \in \mathcal{B}}$, with

$$S^{-b} = -S^b, \quad \partial S^b \perp ((0, T) \times \Omega) = 0.$$

- (6) Dislocation system at time t : $(T^b(t))_b$ with $T^b(t) := \mathbf{p}_*(S^b|_t)$.
- (7) Thickened slip trajectories $\Sigma_\eta := (S_\eta^b)_b$, where $S_\eta^b := \eta * S^b$ with η a smooth and compactly supported dislocation line profile $\eta : \mathbb{R}^3 \rightarrow [0, \infty)$ satisfying $\int \eta \, dx = 1$.

(8) Geometric slip rate:

$$g^b(t, \cdot) := \eta * \left[\frac{D}{Dt} S^b(t, \cdot) \times \bar{T}^b(t, \cdot) m^b \right].$$

with m^b the multiplicity of $T^b(t)$ and the dislocation velocity

$$\frac{D}{Dt} S^b(t, x) := \frac{\mathbf{p}(\xi^b(t, x))}{|\mathbf{t}(\xi^b(t, x))|},$$

where

$$\xi^b(t, x) := \frac{\nabla^{S^b} \mathbf{t}(t, x)}{|\nabla^{S^b} \mathbf{t}(t, x)|}$$

is the geometric derivative. This ξ^b can equivalently be defined as the unique vector such that $\mathbb{T}_{(t,x)} S^b = \text{span}\{\bar{T}^b(t, x), \xi^b(t, x)\}$ and such that $\xi^b(t, x)$ is pointing “forward in time”, i.e., $\mathbf{t}(\xi^b(t, x)) = \xi^b(t, x) \cdot \mathbf{e}_0 \geq 0$.

(9) Regularity (no horizontal pieces): $\mathbf{t}(\xi^b(t, x)) = \xi^b(t, x) \cdot \mathbf{e}_0 > 0$.

(10) Plastic flow equation:

$$\dot{P} = -Q^{-1} \dot{Q} Q^{-1} = D,$$

where the total plastic drift is given as

$$D(t, x) := \int b \otimes g^b(t, x) \, d\mathbf{k}(b).$$

(11) Total energy:

$$\mathcal{E}(t, y, Q, \Phi) := \mathcal{W}_e(y, Q) - \int f(t) \cdot y \, dx,$$

where $f: [0, T] \times \Omega \rightarrow \mathbb{R}^3$ is the external bulk loading and the elastic energy is given as

$$\mathcal{W}_e(y, Q) := \int_{\Omega} W_e(\nabla y Q) \, dx,$$

with $W_e: \Omega \times \text{GL}^+(3) \rightarrow \mathbb{R}$ the (frame-indifferent) elastic energy density.

(12) Piola–Kirchhoff stress (referential elastic stress), Mandel stress (structural plastic stress), and referential configurational stress:

$$\begin{aligned} T &:= DW_e(\nabla y Q) Q^T, \\ M &:= Q^T \nabla y^T DW_e(\nabla y Q), \\ X^b &:= Q M^T b, \quad b \in \mathcal{B}. \end{aligned}$$

(13) Elastic force balance:

$$\rho \ddot{y} - \text{Div}[DW_e(\nabla y Q) Q^T] = f.$$

(14) Flow rule (Biot inclusion):

$$PX^b \in \partial R^b(Q^T g^b), \quad b \in \mathcal{B},$$

with the dissipation potential $R^b: \mathbb{R}^3 \rightarrow [0, +\infty]$ satisfying:

R^b is proper ($\neq +\infty$), convex, lower semicontinuous, $R^b(0) = 0$;

the symmetry relation $R^{-b}(-\xi) = R^b(\xi)$ holds for all $b \in \mathcal{B}$;

$\xi \cdot \partial R^b(\xi) > 0$ (element-wise) for non-zero $\xi \in \mathbb{R}^3$;

If $b \otimes \xi \notin \mathfrak{p}$ for $\xi \in \mathbb{R}^3$, then $R^b(\xi) = +\infty$.

6. FURTHER EFFECTS AND OUTLOOK

In this section we outline how further physical effects may be incorporated into our model, and describe various directions for future work.

6.1. Elastic equilibrium. Let us consider the consequences of imposing the following further assumption:

Inertial effects can be neglected.

This is a common hypothesis in both macroscopic plasticity modeling and many micromechanical approaches to dislocation motion. The main theoretical justification for assuming this is that the frictional forces for dislocation motion dominate inertial effects in any slow-loading process [15].

In order to formulate the resulting equations, we further need a qualitative relationship between elastic and plastic motion, for which we assume:

Elastic relaxation occurs on a much faster timescale than plastic flow.

Experiments suggest that this is a reasonable assumption in many circumstances, see for example [12, 13]. It is also theoretically consistent (at least for metals) since the flow of dislocations is constricted to be always slower than the propagation of elastic distortion through shear waves (S-waves), because plastic drag tends to infinity as the plastic distortion rate approaches the shear wave speed; see [30]. In this case, we obtain that the **elastic equilibrium equation** (where the inertial term has been dropped)

$$-\operatorname{Div} T = -\operatorname{Div}[D W_e(\nabla_y Q) Q^T] = f$$

is always satisfied, even during plastic flow. In other words, the evolution is *quasi-static* (see, e.g., [83] for quasi-static evolution). If the material is hyperelastic, then this is equivalent to $y(t)$ being a minimizer of $\mathcal{E}(t, \cdot, Q(t))$ for all t .

6.2. Dislocation climb. If we wanted to dispense with the plastic incompressibility assumption in order to allow climb as well as glide, then we need to define the total plastic drift in (3.10) instead as follows:

$$D(t, x) := \int b \otimes \operatorname{proj}_{\langle Q(t, x)b \rangle^\perp} g^b(t, x) \, d\kappa(b),$$

where by $\operatorname{proj}_{\langle Q(t, x)b \rangle^\perp}$ we denote the orthogonal projection onto the orthogonal complement of the line $Q(t, x)b$. This ensures that $\operatorname{tr}(QD) = 0$ and so the scaffold Q remains in $\operatorname{SL}(3)$; without this restriction, it is unclear how to interpret the scaffold Q once $\det Q \neq 1$. A natural way to account for the volumetric change caused by climb would be to add a further field describing point defects.

6.3. Rate-independent evolution. Experiments show that plastic flow is *rate-dependent* (viscous), but only slightly so below absolute temperatures of approximately $0.35\vartheta_m$, where ϑ_m is the melting temperature of the material, see [45, Section 78]. For instance, in a commonly-used power viscosity law, see Example 4.2 and also [70, Section 5.4], the stress depends on the rate with exponent $1/N$, that is, $DR(\xi) \sim |\xi|^{1/N}$. For example, steel with 35% carbon at 450 °C has $N = 15$ and the titanium-aluminium alloy TA6V at 350 °C has $N = 120$; more values can be found in [70, Table 6.2]. The movement of the system is directed in such a way as to move the stress toward the yield surface, where the movement stops as the internal friction stress threshold is no longer exceeded. It can be seen that the larger N is, the faster this “plastic relaxation” takes place.

On “slow” time scales we should therefore see near-infinitely fast relaxation, i.e. $PX^b \in \mathcal{S}^b$ always, which is called (*local*) *stability*. A basic assumption in the present theory is that the system evolves according to a flow rule as defined above. However, if f were to be held constant at some point in time, the system would settle very quickly into a rest state until the external loading changes and the system is pushed out of equilibrium. The traditional rate-independent modeling is built upon the assumption that only this global movement is interesting and the fast “relaxation” movements towards a rest state can be neglected, at least if the system does not jump to a far-away state in an instant.

A further key question, which is also central in other recent works [28, 29, 78, 79, 81, 82, 88, 98], is whether during a jump at “infinite” speed the modeling assumption of rate-independence can be upheld. Most materials in fact display rate-dependent behavior under fast deformations. We do not pursue this question further here.

The work [95] will implement a rate-independent version of the model presented here, which relies on a number of further technicalities and a reformulation of the flow rule into a stability inequality and an energy balance.

6.4. Core energy. To incorporate the fact that the energy of a dislocation may not exclusively be captured via the elastic energy, one may also add a **core energy** for the dislocation system $\Phi = (T^b)_b$ to the total energy. This expresses an additional chemical potential energy in the system due to the fact that dislocation configurations are energetically unfavourable in comparison to the undistorted lattice on an *atomistic* level. It does *not* model the elastic potential energy “trapped” in the elastic distortion, which cannot be released since $\text{curl}P \neq 0$ at a dislocation (this effect is included automatically).

A simple model for the core energy is

$$\mathcal{W}_c(\Phi) := \zeta \int \mathbf{M}(T^b) \, d\kappa(b),$$

where $\zeta > 0$ is a material constant and $\mathbf{M}(T^b)$ is the total length of the dislocations with Burgers vector b . More complicated expressions (e.g., with anisotropy or b -dependent ζ) are of course possible, as in [11].

Using the simple core energy above, the total energy is then modified from (4.3) to

$$\mathcal{E}(t, y, Q, \Phi) := \mathcal{W}_e(y, Q) - \int f(t) \cdot y \, dx + \mathcal{W}_c(\Phi)$$

and the plastic force balance (4.6) would also need to incorporate a *curvature*-type term.

6.5. Hardening and softening. In its most general form, hardening or softening describe the processes by which the *effective* elastic stability domain changes, in particular expands or contracts, due to a change in the internal state of the specimen. Hardening is usually anisotropic and due to a variety of microscopic effects like dislocation entanglement. We discuss some connections to existing models and approaches here.

One simple way to add hardening to our model is to add a prefactor to the dissipational cost Diss , which depends on P or further internal variables. This is the approach taken in [95] and we refer to that work for one possible way to implement hardening effects that yields a mathematically well-posed theory.

Another, more classical, way is to add a “hardening energy” to the total energy, which depends on further internal variables. Then, one encounters another (generalized) stress, which is power-conjugate to the rate of change in the internal variables. We denote the state space of the additional internal variables by \mathfrak{Z} and the corresponding state by $z = z(t, x)$. For simplicity we assume that \mathfrak{Z} has a linear structure, so that \dot{z} is the rate of change for z (if \mathfrak{Z} had a Lie group structure, we could mimick the previous development for P and consider the internal variable drift $\dot{z}z^{-1}$ in the structural frame or $z^{-1}\dot{z}$ in the referential frame; see [78] for more on this approach). We then add a **hardening energy**

$$\mathcal{W}_h(z) := \int_{\Omega} W_h(z(x)) \, dx$$

with $W_h: \mathfrak{Z} \rightarrow [0, \infty)$, to our total energy. The flow rule now involves the plastic as well as the internal rates and stresses, and hence the signature of R^b has to be suitably adapted.

In **isotropic hardening**, the elastic stability domain \mathcal{S}^b ($b \in \mathcal{B}$) remains centered around the origin but can expand in what is called **positive hardening** and contract in **negative hardening** or **softening**. In **kinematic hardening**, the elastic stability domain is translated. Combined, these two effects give a first approximation to the often-observed phenomenon that an increase in tensile

yield strength goes along with a decrease in compressive yield strength, called the **Bauschinger effect**, which, however, in general is more complex, see for instance [70, Section 3.3.7] and [56].

Example 6.1. In the often-considered **von Mises isotropic–kinematic hardening**, the elastic stability domain \mathcal{S}^b depends on two internal variables, $H^b \in \mathfrak{p}^* \subset \mathbb{R}^{3 \times 3}$ and $\zeta^b \in \mathbb{R}$, called **back-stresses**. Then, the elastic stability domain is prescribed to be

$$\mathcal{S}^b = \left\{ \sigma = (\sigma^b, H^b, \zeta^b) : |\text{dev}(\sigma^b - H^b)| + \zeta^b - \frac{2}{3}\sigma_0^b \leq 0 \right\},$$

where $\sigma_0^b > 0$ is a constant (the initial tensile yield strength) and, as usual, $|A| = |A|_F = [\text{tr}(A^T A)]^{1/2}$ is the Frobenius norm. This means that the elastic stability domain is translated with H^b and dilated with ζ^b . Using a different matrix norm, one can get different shapes of the yield surface.

Other hardening models (e.g., Tresca, Mohr–Coulomb or Drucker–Prager) could likewise be incorporated; we refer to [46, p.66 ff.] for descriptions of these effects.

6.6. Coarse-graining. Our model falls into the category of “semi-discrete” dislocation models, which occupy a position on length-scales above fully discrete lattice models like those studied in [4, 5, 10, 50, 52–54, 91, 108] since we have effectively let the lattice spacing tend to zero. It would be interesting to investigate if this relationship can be made rigorous.

On the other hand, our model works with length-scales below typical plasticity models since we still account for individual dislocation lines. One advantage of the mathematical machinery which comes with using currents is that it also immediately suggests methods to enable passage from a model representing individual dislocation lines to *fields* of dislocation lines. As real materials usually contain huge numbers of dislocation lines, with total length per unit volume usually around 10^{10} m^{-2} to 10^{12} m^{-2} in well-annealed crystals and up to 10^{15} m^{-2} after heavy plastic distortion, see [55], it is a sensible mathematical abstraction to pass to a coarse-grained continuum of lines. The latter fields are representable by *normal currents*. Normal currents have slices and a boundary operator, so the modeling generalizes with very few modifications. Indeed, this is in keeping with various results on the coarse-graining of dislocation models in lower dimensions [19, 31, 40, 41, 84, 102, 107]. The present framework also allows for the creation of new dislocation lines from point defects, which we assume to be so frequent that this creation can essentially appear anywhere (recall that out currents sit in a mesoscale between the atomistic and macroscopic scales). We leave further investigations into coarse-graining for future work.

APPENDIX A. RIGOROUS GEOMETRIC SETTING

In this appendix we rigorously define some notions and give a more precise treatment of the geometry of dislocations and slip trajectories. We also prove (still on a mostly formal level) some statements used in our derivation. A fully rigorous treatment can be found in [95, 96].

A.1. Linear and multilinear algebra. As usual, we equip \mathbb{R}^3 with its standard inner product, $u \cdot v = \sum_i u^i v^i$ where u^i, v^i are the components of the vectors $u, v \in \mathbb{R}^3$. We also employ the standard orthonormal basis for this space, so that $\mathbb{R}^3 = \text{span}\{e_1, e_2, e_3\}$. A key aspect of our approach is to consider the motion of dislocations in (Galilean) space-time, which we represent as $\mathbb{R} \times \mathbb{R}^3 \cong \mathbb{R}^{1+3}$. This space is again endowed with the usual inner product and its canonical orthonormal basis so that $\mathbb{R}^{1+3} = \text{span}\{e_0, e_1, e_2, e_3\}$, where we abuse notation by identifying e_1, e_2 and e_3 with their natural extensions to this space, and $e_0 = (1, 0, 0, 0)$ is the additional basis vector pointing in the (positive) time direction. It will be convenient to denote the orthogonal projection onto the “time” component by $\mathbf{t}: \mathbb{R}^{1+3} \rightarrow \mathbb{R} \times \{0\}^3 \cong \mathbb{R}$ and the orthogonal projection onto the “space” component by $\mathbf{p}: \mathbb{R}^{1+3} \rightarrow \{0\} \times \mathbb{R}^3 \cong \mathbb{R}^3$. We also write the natural linear extensions of these projections to multi-vectors (which we define below) using the same symbols.

The space of matrices $\mathbb{R}^{m \times n}$ comes with the Frobenius inner product

$$A : B := \sum_{i,j} A_j^i B_j^i = \text{tr}(A^T B) = \text{tr}(B^T A),$$

where upper indices indicate rows and lower indices indicate columns. As matrix norm we use the induced Frobenius norm, i.e., $|A| := (A : A)^{1/2} = [\text{tr}(A^T A)]^{1/2}$.

Throughout the following, let $k = 0, 1, 2, \dots, n$. We recall that the **exterior** or **wedge product**, denoted \wedge , is an anti-commutative algebraic operation which is used to study the geometry of subspaces of a vector space. In particular, the linear combinations of the k -fold products of vectors from \mathbb{R}^n form the vector space of k -**vectors** $\wedge_k \mathbb{R}^n$. Its dual space, the set of k -**covectors**, is $\wedge^k \mathbb{R}^n$ and the duality product between these space is denoted by $\langle \cdot, \cdot \rangle : \wedge_k \mathbb{R}^n \times \wedge^k \mathbb{R}^n \rightarrow \mathbb{R}$. We recall that it is canonical to identify $\wedge_0 \mathbb{R}^n = \wedge^0 \mathbb{R}^n = \mathbb{R}$ as just being the real scalars. Given the canonical bases $\{e_1, e_2, e_3\}$ of $\mathbb{R}^3 \cong \wedge_1 \mathbb{R}^3$ and $\{e_0, e_1, e_2, e_3\}$ of $\mathbb{R}^{1+3} \cong \wedge_1 \mathbb{R}^{1+3}$, we denote the natural dual bases of $\wedge^1 \mathbb{R}^3$ and $\wedge^1 \mathbb{R}^{1+3}$ as $\{dx^1, dx^2, dx^3\}$ and $\{dx^0, dx^1, dx^2, dx^3\}$, respectively, which are characterized via the relations

$$\langle e_i, dx^j \rangle = \begin{cases} 1 & \text{if } i = j, \\ 0 & \text{otherwise.} \end{cases}$$

Given the distinguished nature of the time direction in our modeling, we will also write $dt := dx^0$.

A k -vector $\eta \in \wedge_k \mathbb{R}^n$ is called **simple** if it can be written as a single k -fold wedge product, $\eta = v_1 \wedge \dots \wedge v_k$ with $v_\ell \in \mathbb{R}^n$, and likewise for k -covectors. The spaces of vectors and covectors have inner products which arise naturally from the inner product of the underlying space. For simple k -vectors $\eta = v_1 \wedge \dots \wedge v_k$ and $\xi = w_1 \wedge \dots \wedge w_k$ this inner product is

$$(\eta, \xi) = \det \begin{pmatrix} v_1 \cdot w_1 & \cdots & v_1 \cdot w_k \\ \vdots & \ddots & \vdots \\ v_k \cdot w_1 & \cdots & v_k \cdot w_k \end{pmatrix},$$

which is extended to general k -vectors by linearity. A similar construction applies for k -covectors.

As norms on the spaces $\wedge_k \mathbb{R}^n$ and $\wedge^k \mathbb{R}^n$ we use the so-called **mass** and **comass norms** of $\eta \in \wedge_k \mathbb{R}^n$ and $\alpha \in \wedge^k \mathbb{R}^n$ instead of the norms induced by the inner products defined above. These norms are

$$|\eta| := \sup \{ |\langle \eta, \alpha \rangle| : \alpha \in \wedge^k V, |\alpha| = 1 \}, \\ |\alpha| := \sup \{ |\langle \eta, \alpha \rangle| : \eta \in \wedge_k V \text{ simple, unit} \}.$$

Here, a simple k -vector $\eta = v_1 \wedge \dots \wedge v_k$ is called a **unit** if $\{v_\ell\}_\ell$ can be chosen as an orthonormal system.

For $\eta \in \wedge_k \mathbb{R}^n$ and $\alpha \in \wedge^l \mathbb{R}^n$ we further define the **restriction operators** $\eta \lrcorner \alpha \in \wedge^{l-k} \mathbb{R}^n$ and $\eta \llcorner \alpha \in \wedge_{k-l} \mathbb{R}^n$ via

$$\langle \xi, \eta \lrcorner \alpha \rangle := \langle \xi \wedge \eta, \alpha \rangle, \quad \xi \in \wedge_{l-k} \mathbb{R}^n, \\ \langle \eta \llcorner \alpha, \beta \rangle := \langle \eta, \alpha \wedge \beta \rangle, \quad \beta \in \wedge^{k-l} \mathbb{R}^n.$$

A simple k -vector $\eta \in \wedge_k \mathbb{R}^n$ represents an oriented k -plane in \mathbb{R}^n . For instance, $\eta = v_1 \wedge \dots \wedge v_k \in \wedge_k \mathbb{R}^n$ can be thought of as the k -plane $R := \text{span } \eta := \text{span}\{v_1, \dots, v_k\}$ together with the orientation induced by the ordering of v_1, \dots, v_k (any other basis of R has the same orientation if and only if the change-of-base matrix has positive determinant). Another way to describe an oriented k -plane is by providing a unit “normal” $(n-k)$ -plane $S := \text{span } \xi$ with $\xi \in \wedge_{n-k} \mathbb{R}^n$ and setting $R := S^\perp$ (with an “orthogonal orientation”). These two approaches are related via Hodge duality as follows: For a k -vector $\eta \in \wedge_k \mathbb{R}^n$ in the cases $n = 3$ or $n = 4$ we consider here, we define the **Hodge dual** $\star \eta \in \wedge_{n-k} \mathbb{R}^n$ as the unique vector satisfying, respectively,

$$\xi \wedge \star \eta = (\xi, \eta) e_1 \wedge e_2 \wedge e_3 \quad \text{or} \quad \xi \wedge \star \eta = (\xi, \eta) e_0 \wedge e_1 \wedge e_2 \wedge e_3$$

for all $\xi \in \wedge_k \mathbb{R}^n$. For k -covectors $\alpha \in \wedge^k \mathbb{R}^n$ we may use the same formulae to define $\star \alpha \in \wedge^{n-k} \mathbb{R}^n$, with $e_1 \wedge e_2 \wedge e_3$ replaced by $dx^1 \wedge dx^2 \wedge dx^3$ and $e_0 \wedge e_1 \wedge e_2 \wedge e_3$ replaced by $dt \wedge dx^1 \wedge dx^2 \wedge dx^3$. One can observe that, applied to a k -vector or k -covector, the inverse of the Hodge star is given as

$$\star^{-1} = (-1)^{k(n-k)} \star, \quad (\text{A.1})$$

and it may further be checked that a natural duality rule holds:

$$\langle \star \xi, \star \alpha \rangle = \langle \xi, \alpha \rangle, \quad \xi \in \wedge_k \mathbb{R}^n, \alpha \in \wedge^k \mathbb{R}^n.$$

In the special case $n = 3$ we also have the following geometric interpretation of the Hodge dual of a 2-vector: For $\eta \in \wedge_2 \mathbb{R}^3$, its dual $\star \eta$ is the (1-)vector normal to any two-dimensional hyperplane with orientation η . Moreover, for $a, b \in \wedge_1 \mathbb{R}^3 \cong \mathbb{R}^3$ the identities

$$\star(a \times b) = a \wedge b, \quad \star(a \wedge b) = a \times b \quad (\text{A.2})$$

hold, where “ \times ” denotes the classical vector cross product in \mathbb{R}^3 . Indeed, for any $v \in \wedge_1 \mathbb{R}^3$, the triple product $v \cdot (a \times b)$ is equal to the determinant $\det(v, a, b)$ of matrix with columns v, a, b , and so

$$v \wedge \star(a \times b) = v \cdot (a \times b) e_1 \wedge e_2 \wedge e_3 = \det(v, a, b) e_1 \wedge e_2 \wedge e_3 = v \wedge (a \wedge b).$$

Hence, the first identity in (A.2) follows. The second identity follows by applying \star on both sides and using $\star^{-1} = \star$ (this is (A.1) with $n = 3$ and $k = 1$). Note that no similar representation of a 2-plane by a normal vector holds in \mathbb{R}^4 since the Hodge dual of a 2-vector in \mathbb{R}^4 is again a 2-vector.

Occasionally, we use the k -times **wedge product of a linear map**, particularly in the case of the projections \mathbf{t} and \mathbf{p} defined above. If $S \in \mathcal{L}(\mathbb{R}^n; \mathbb{R}^N)$, we let $\wedge^k S \in \mathcal{L}(\wedge^k \mathbb{R}^n; \wedge^k \mathbb{R}^N)$ be the unique linear map for which

$$\wedge^k S(v_1 \wedge \cdots \wedge v_k) = S v_1 \wedge \cdots \wedge S v_k, \quad v_1, \dots, v_k \in \mathbb{R}^n;$$

then we extend by multi-linearity to all of $\wedge^k S$. For reasons of convenience, we will still write simply S for $\wedge^k S$.

A.2. Normal and integral currents. The theory of currents will provide us with a precise mathematical language to describe dislocations and slip trajectories. For details and proofs of the following statements we refer to [58] or the monolithic [37].

Given an open set $U \subseteq \mathbb{R}^n$ and $k = \{0\} \cup \mathbb{N}$, we let $\mathcal{D}^k(U)$ be the space of (**smooth**) **differential k -forms** with compact support in U , that is, $\mathcal{D}^k(U) := C_c^\infty(U; \wedge^k \mathbb{R}^n)$. As with vectors and covectors, a k -form is called **simple** if it takes simple k -covector as values everywhere. The **exterior differential** of $\omega \in \mathcal{D}^k(U)$ is the $(k+1)$ -form $d\omega \in \mathcal{D}^{k+1}(U)$ defined inductively as follows: For a 0-form $f \in \mathcal{D}^0(U) = C_c^\infty(U; \mathbb{R})$, we set

$$df := \sum_i \frac{\partial f}{\partial x^i} dx^i \in \mathcal{D}^1(U),$$

where we recall from Section A.1 that dx^i is the i th element of the dual canonical basis. Then, for a simple k -form which can be expressed as $\omega = f dx^{j_1} \wedge \cdots \wedge dx^{j_k}$ we inductively set $d\omega := (df) \wedge dx^{j_1} \wedge \cdots \wedge dx^{j_k}$. For a more general k -form, this definition is then extended by linearity.

Just like in the theory of Schwartz distributions, currents are constructed by duality: Indeed, the elements of the dual space $\mathcal{D}_k(U) := \mathcal{D}^k(U)^*$ are called (**de Rham**) **k -currents**. This space is equipped with a natural **boundary operator**, which for k -current $T \in \mathcal{D}^k(\mathbb{R}^n)$, $k \geq 1$, is defined as the $(k-1)$ -current $\partial T \in \mathcal{D}_{k-1}(\mathbb{R}^n)$ with

$$\langle \partial T, \omega \rangle := \langle T, d\omega \rangle, \quad \omega \in \mathcal{D}^{k-1}(\mathbb{R}^n).$$

For a 0-current T , one formally sets $\partial T := 0$.

We think of k -currents as generalized k -surfaces; we note that there is an alternative view on k -currents as “distributional”, that is, very rough, differential forms, but for us this is not relevant. The point of view we take is particularly pertinent for the following subclass of currents: A (local)

Borel measure $T \in \mathcal{M}_{\text{loc}}(\mathbb{R}^n; \wedge_k \mathbb{R}^n)$ (i.e., with values in the space $\wedge_k \mathbb{R}^n$ of k -vectors) is called an **integer-multiplicity rectifiable k -current** ($k \in \mathbb{N} \cup \{0\}$) if it is of the form

$$T = m \vec{T} \mathcal{H}^k \llcorner R,$$

that is, T is an element of the dual space to the space $\mathcal{D}^k(\mathbb{R}^n)$ of k -forms via

$$\langle T, \omega \rangle = \int_R \langle \vec{T}(x), \omega(x) \rangle m(x) \, d\mathcal{H}^k(x), \quad \omega \in \mathcal{D}^k(\mathbb{R}^n),$$

where

- (i) $R \subset \mathbb{R}^n$ is countably \mathcal{H}^k -rectifiable with $\mathcal{H}^k(R \cap K) < \infty$ for all compact sets $K \subset \mathbb{R}^n$;
- (ii) $\vec{T}: R \rightarrow \wedge_k \mathbb{R}^n$ is \mathcal{H}^k -measurable and for \mathcal{H}^k -a.e. $x \in R$ the k -vector $\vec{T}(x)$ is simple, has unit length ($|\vec{T}(x)| = 1$), and lies in the approximate tangent space $T_x R$ to R at x ;
- (iii) $m: R \rightarrow \mathbb{N}$ is locally $(\mathcal{H} \llcorner R)$ -integrable.

The k -vector field \vec{T} is called the **orientation map** of T and m is the **multiplicity**. Here, we do not recall precisely the notion of the k -dimensional Hausdorff (outer) measure \mathcal{H}^k and (countably) k -rectifiable sets (see again [37, 58] or [6] for this). Intuitively, one can think of an integer-multiplicity rectifiable k -current as a collection of (oriented) k -dimensional C^1 - or Lipschitz-manifolds, which may overlap and thus have a multiplicity other than 1.

We further have the **Radon–Nikodým decomposition**

$$T = \vec{T} \|T\|,$$

where \vec{T} is the orienting map as above and $\|T\| = m \mathcal{H}^k \llcorner R \in \mathcal{M}^+([0, T] \times \mathbb{R}^3)$ is the **total variation measure**. The (global) mass of T is

$$\mathbf{M}(T) = \|T\|(\mathbb{R}^n) = \int_R m(x) \, d\mathcal{H}^k(x).$$

Now, define the following classes of **integral k -currents** ($k \in \mathbb{N} \cup \{0\}$):

$$\begin{aligned} \mathbf{I}_k(\mathbb{R}^n) &:= \{ T \text{ integer-multiplicity rectifiable } k\text{-current} : \mathbf{M}(T) + \mathbf{M}(\partial T) < \infty \}, \\ \mathbf{I}_k(\overline{\Omega}) &:= \{ T \in \mathbf{I}_k(\mathbb{R}^n) : \text{supp } T \subset \overline{\Omega} \}. \end{aligned}$$

By the so-called boundary rectifiability theorem, see [37, 4.2.16] or [58, Theorem 7.9.3], for $T \in \mathbf{I}_k(\overline{\Omega})$, also $\partial T \in \mathbf{I}_{k-1}(\overline{\Omega})$.

We also briefly recall the theory of pushforwards of integral currents. Let $\theta: \overline{\Omega} \rightarrow \mathbb{R}^n$ be smooth and let $T = m \vec{T} \mathcal{H}^k \llcorner R \in \mathbf{I}_k(\overline{\Omega})$. The **(geometric) pushforward** $\theta_* T$ (often denoted by “ $\theta_{\#} T$ ” in the geometric measure theory literature) is defined via

$$\langle \theta_* T, \omega \rangle := \langle T, \theta^* \omega \rangle, \quad \omega \in \mathcal{D}^k(\mathbb{R}^n),$$

where $\theta^* \omega$ denotes the pullback of the k -form ω . If $\theta|_{\text{supp } T}$ is **proper**, i.e., $\theta^{-1}(K) \cap \text{supp } T$ is compact for every compact $K \subset \mathbb{R}^n$, then $\theta_* T \in \mathbf{I}_k(\overline{\theta(\Omega)})$, see, for instance, [58, (3) on p.197]. If we denote the approximate derivative of θ (which is defined almost everywhere) with respect to the k -rectifiable set R carrying T by $D^R \theta$ (i.e. $D^R \theta$ is the restriction of $D\theta$ to $T_x R$), then

$$\langle \theta_* T, \omega \rangle = \int \langle D^R \theta(\vec{T}(x)), \omega(\theta(x)) \rangle d\|T\|(x), \quad \omega \in \mathcal{D}^k(\mathbb{R}^n).$$

It also holds that

$$\partial(\theta_* T) = \theta_*(\partial T). \tag{A.3}$$

Finally, the slicing theory of integral currents (see [58, Section 7.6] or [37, Section 4.3]) allows one to define the “restriction” of a given integral current $S = m \vec{S} \mathcal{H}^{k+1} \llcorner R \in \mathbf{I}_{k+1}(\overline{\Omega})$ to a level set of a Lipschitz map $f: \mathbb{R}^n \rightarrow \mathbb{R}$ (for us, this will always be the temporal projection $\mathbf{t}(t, x) := t$) as follows: Set $R|_t := f^{-1}(\{t\}) \cap R$. Then, $R|_t$ is (countably) \mathcal{H}^k -rectifiable for almost every $t \in \mathbb{R}$ and for \mathcal{H}^k -almost every $z \in R|_t$ (if $f = \mathbf{t}$, then $z = (t, x)$), the approximate tangent spaces $T_z R$

and $T_z R|_t$, as well as the approximate gradient $\nabla^R f(z)$ (the projection of $\nabla f(z)$ onto $T_z R$) exist. Furthermore,

$$T_z R = \text{span}\{T_z R|_t, \xi(z)\}, \quad \xi(z) := \frac{\nabla^R f(z)}{|\nabla^R f(z)|} \perp T_z R|_t.$$

Also, $\xi(z)$ is simple and has unit length. If we set

$$m_+(z) := \begin{cases} m(z) & \text{if } \nabla^R f(z) \neq 0, \\ 0 & \text{otherwise,} \end{cases} \quad \xi^*(z) := \frac{D^R f(z)}{|D^R f(z)|},$$

where $D^R f(z)$ is the restriction of the differential $Df(z)$ to $T_z R$, and

$$\vec{S}|_t(z) := \vec{S}(z) \lrcorner \xi^*(z) \in \wedge_k T_z R|_t \subset \wedge_k T_z R,$$

then we may define the **slice** of S with respect to f at t via

$$S|_t := m_+ \vec{S}|_t \mathcal{H}^k \lrcorner R|_t.$$

It can be shown that $S|_t$ is an integral k -current satisfying in particular the following properties:

(i) *The coarea formula for slices:*

$$\int_R g |\nabla^R f| \, d\mathcal{H}^{k+1} = \int \int_{R|_t} g \, d\mathcal{H}^k \, dt \quad (\text{A.4})$$

holds for all $g: R \rightarrow \mathbb{R}^N$ that are \mathcal{H}^{k+1} -measurable and integrable on R .

(ii) *The mass decomposition:*

$$\int \mathbf{M}(S|_t) \, dt = \int_R |\nabla^R f| \, d\|S\|.$$

(iii) *The cylinder formula:*

$$S|_t = \partial(S \lrcorner \{f < t\}) - (\partial S) \lrcorner \{f < t\}.$$

(iv) *The boundary formula:*

$$\partial S|_t = -(\partial S)|_t.$$

A.3. Description of dislocations and slip trajectories via integral currents. Our modeling of dislocations is made rigorous as follows: All dislocation lines with structural Burgers vector $b \in \mathcal{B}$ that are contained in our material body at time $t \in [0, T]$, are collected in a 1-dimensional integral current $T^b(t)$ in Ω (see [24, 25, 101] for similar approaches). This current is boundaryless in Ω , i.e.,

$$\partial T^b(t) \lrcorner \Omega = 0$$

because dislocation lines are always closed loops inside the specimen Ω . Moreover, since one may flip the sign of a Burgers vector when at the same time also reversing all dislocation line directions, the symmetry relation

$$T^{-b}(t) = -T^b(t)$$

needs to hold for the family $(T^b(t))_{b \in \mathcal{B}}$ and (almost) every $t \in [0, T]$.

The associated **slip trajectories** likewise can be expressed as 2-dimensional integral currents S^b (for the Burgers vector $b \in \mathcal{B}$) in the space-time cylinder $[0, T] \times \Omega$ with the property that

$$\partial S^b \lrcorner ((0, T) \times \Omega) = 0. \quad (\text{A.5})$$

Moreover, the symmetry relation

$$S^{-b} = -S^b$$

needs to hold for the family $(S^b)_{b \in \mathcal{B}}$, just like it did for the dislocations themselves. In this description of slip trajectories, the **dislocation system** at time t is given by

$$T^b(t) := \mathbf{p}_*(S^b|_t), \quad b \in \mathcal{B}, \quad (\text{A.6})$$

i.e., the pushforward under the spatial projection $\mathbf{p}(t, x) := x$ of the slice $S^b|_t$ of S^b at time t (that is, with respect to the temporal projection $\mathbf{t}(t, x) := t$). The pushforward here moves the slice

from $\{t\} \times \Omega$ to Ω . The slicing theory of integral currents recalled in the previous section entails that $T^b(t)$ is a 1-dimensional integral current in Ω and (A.5) further implies $\partial T^b(t) \llcorner \Omega = 0$ and $T^{-b}(t) = -T^b(t)$ for almost every $t \in (0, T)$ and all $b \in \mathcal{B}$.

The total traversed **slip surface** from $T^b(s)$ to $T^b(t)$ is the integral 2-current in \mathbb{R}^3 given by

$$S^b|_s^t := \mathbf{p}_* [S^b \llcorner ([s, t] \times \Omega)],$$

that is, the pushforward under the spatial projection of the restriction of S^b to the time interval $[s, t]$. However, $S^b|_s^t$ does not contain a “time index”, i.e., a time coordinate, which is needed to define the plastic flow (see Section 3.3). Furthermore, areas that are traversed several times may lead to cancellations in the slip surface $S^b|_s^t$, but not in the slip trajectory S^b itself. These are the fundamental reasons why we work with the space-time slip trajectories and not the slip surfaces in this work.

We further assume that there are no “horizontal parts” in S^b , that is,

$$\|S^b\|(\{t\} \times \Omega) = 0 \quad \text{for a.e. } t \in [0, T]. \quad (\text{A.7})$$

The reason for this is that over such horizontal parts we again lack the “time index” we need to define the plastic evolution (a horizontal piece is essentially just a slip surface that gets traversed instantaneously).

The companion work [96] investigates the notion of space-time trajectories, and in particular the associated notion of *variation* (the simplest form of a dissipation along a slip trajectory) in more detail.

A.4. Dislocation velocity. The dislocation velocity is a natural quantity when considering space-time integral currents: Let us first recall from the slicing theory of integral currents that for \mathcal{L}^1 -almost every $t \in [0, T]$ and $\|S^b|_t\|$ -almost every (t, x) the approximate tangent spaces $\mathbf{T}_{(t,x)} S^b$, $\mathbf{T}_{(t,x)} S^b|_t$ as well as the approximate gradient $\nabla^{S^b} \mathbf{t}(t, x)$ to \mathbf{t} at (t, x) (that is, the orthogonal projection of $\nabla \mathbf{t}(t, x)$ onto $\mathbf{T}_{(t,x)} S$) exist (see, e.g., [58, Lemma 7.6.1 (2)]). Here we also use “ S^b ” in place of its carrier set, i.e., in place of R^b if $S^b = m^b \vec{S}^b \llcorner \mathcal{H}^2 \llcorner R^b$. It also holds that

$$\mathbf{T}_{(t,x)} S^b = \text{span}\{\mathbf{T}_{(t,x)} S^b|_t, \xi^b(t, x)\}, \quad \xi^b(t, x) := \frac{\nabla^{S^b} \mathbf{t}(t, x)}{|\nabla^{S^b} \mathbf{t}(t, x)|} \perp \mathbf{T}_{(t,x)} S|_t.$$

Thus,

$$\vec{S}^b|_t = \vec{S}^b \llcorner \xi^b, \quad \vec{S}^b = \xi^b \wedge \vec{S}^b|_t,$$

where the second equality is a consequence of the general relation $(\xi \wedge \tau) \llcorner \xi^* = \tau$ for any $\tau \in \wedge_k \mathbb{R}^{1+d}$ with $\tau \llcorner \xi^* = 0$ (see [37, 1.5.3]).

In the following we fix t, x as above. We calculate (note $|\xi^b| = 1$)

$$|\nabla^{S^b} \mathbf{t}| = |(\mathbf{e}_0 \cdot \xi^b) \xi^b| = |\xi^b \cdot \mathbf{e}_0| = |(\xi^b \cdot \mathbf{e}_0) \mathbf{e}_0| = |\mathbf{t}(\xi^b)|$$

and (recall $\mathbf{p}(\xi^b) \perp \vec{S}^b|_t$)

$$|\mathbf{p}(\vec{S}^b)| = |\mathbf{p}(\xi^b) \wedge \vec{S}^b|_t| = |\mathbf{p}(\xi^b)|.$$

Since $|\mathbf{t}(\xi^b)|^2 + |\mathbf{p}(\xi^b)|^2 = 1$, we obtain in particular the “Pythagorean” identity

$$|\nabla^{S^b} \mathbf{t}|^2 + |\mathbf{p}(\vec{S}^b)|^2 = 1 \quad \|S\| \text{-a.e.} \quad (\text{A.8})$$

Thus, our definition of the dislocation velocity,

$$\frac{D}{Dt} S^b(t, x) := \frac{\mathbf{p}(\xi^b(t, x))}{|\mathbf{t}(\xi^b(t, x))|} = \frac{\mathbf{p}(\xi^b(t, x))}{|\nabla^{S^b} \mathbf{t}(t, x)|} = \frac{\mathbf{p}(\xi^b(t, x))}{\sqrt{1 - |\mathbf{p}(\vec{S}^b)(t, x)|^2}} \quad (\text{A.9})$$

expresses indeed the velocity of dislocation motion.

A.5. Infinitesimal plastic shear. In this section we provide an alternative, more precise, derivation of the formula for the infinitesimal plastic shear (3.4), which takes into account the transformation of planes between the reference configuration and the structural space.

Consider an open and bounded mesoscopic reference domain $U \subset \Omega$, where “mesoscopic” means that atomistic effects can be neglected, but the deformation is nearly constant in U . Assume without loss of generality that $0 \in U$ and that U is partitioned into two parts by an oriented hyperplane H . We describe the hyperplane H by a 2-vector $\mathbf{v} \in \wedge_2 \mathbb{R}^3$ and its associated (oriented) normal vector by $N = \star \mathbf{v}$, where \star is the Hodge star.

Fix a (structural) Burgers vector $b \in \mathcal{B}$ and assume that we are investigating a slip trajectory S^b such that the dislocations at any time $t \in [0, T]$, i.e., $T^b(t) = \mathbf{p}_*(S^b|_t)$, lie entirely in the hyperplane H . Locally, this situation describes the general picture with H being (the spatial restriction of) the approximate tangent space to S^b at a point $(t_0, x_0) \in (0, T) \times \Omega$. Up to time t , the dislocations in S^b traverse the restricted slip trajectory $S^b \llcorner ([0, t] \times U)$. At time t , the dislocations are at the leading edge of S^b , i.e., $T^b(t) = \partial[S^b \llcorner ([0, t] \times U)] + T_0^b$, where T_0^b are the dislocations at the beginning of the evolution represented by S^b .

Assume first that H is precisely the lattice plane dual to the bond q_i (the i 'th scaffold vector), which is the plane with orientation $q_j \wedge q_k$ such that ijk is an even permutation of 123, meaning that $\mathbf{v} = q_j \wedge q_k$ (e.g., if we are considering the bond q_1 , then the dual plane is $\mathbf{v} = q_2 \wedge q_3$). As the dislocation moves, the i 'th bond is translated by the opposite of the structural Burgers vector b . Thus, since the q_i are expressed in referential coordinates, q_i is mapped to $q_i - Qb$. For any other (referential) vector w we posit that only the part of w in direction q_i gets translated by the corresponding fraction of Qb . Furthermore, if H is not aligned with a lattice plane, then we assume that H is linearly decomposed into a sum of its components in the lattice planes $q_j \wedge q_k$ for $j \neq k$ (the decomposition is with respect to the linear structure of $\wedge_2 \mathbb{R}^3$) and the above translation happens separately for all these lattice planes. Summing up, a (referential) vector w is transformed by the dislocations into

$$w' := w - (Qb)\alpha(\mathbf{v}, w), \quad (\text{A.10})$$

where $\alpha = \alpha_{t,x}: \wedge_2 \mathbb{R}^3 \times \mathbb{R}^3 \rightarrow \mathbb{R}$ has the following properties:

$$\begin{cases} \alpha(\cdot, \cdot) \text{ is bilinear;} \\ \alpha(q_j \wedge q_k, q_\ell) = \delta_{\ell i} \text{ for } ijk \text{ an even permutation of } 123. \end{cases} \quad (\text{A.11})$$

We collect the scaffold vectors q_1, q_2, q_3 at (t, x) into the matrix $Q := (q_1, q_2, q_3)$ (as columns), which by the assumed plastic incompressibility (see Section 2.5) satisfies $\det Q = 1$. Then, we claim that the (unique) map α that satisfies the properties given in (A.11) is

$$\alpha(\xi, \mathbf{v}) = [Q^{-T} \star Q^{-1} \xi]^T \mathbf{v} = (\star \xi)^T \mathbf{v}, \quad \xi \in \wedge_2 \mathbb{R}^3, \mathbf{v} \in \mathbb{R}^3. \quad (\text{A.12})$$

Here, the middle expression is to be bracketed from the right, i.e., $Q^{-T}(\star(Q^{-1}\xi))$. The first equality follows simply because this expression for α (uniquely) satisfies the conditions in (A.11), as can be easily checked. To see the equality between the second and third expression in (A.12), we argue as follows: First observe that any simple 3-vector $\zeta = z_1 \wedge z_2 \wedge z_3$ in \mathbb{R}^3 can be written as $\det(z_1, z_2, z_3)E$ with $E := e_1 \wedge e_2 \wedge e_3$, and hence

$$Q^T \zeta = (Q^T z_1) \wedge (Q^T z_2) \wedge (Q^T z_3) = \det(Q^T z_1, Q^T z_2, Q^T z_3)E = \det Q \cdot \det(z_1, z_2, z_3)E = \zeta$$

since $\det Q = 1$ by the assumed plastic incompressibility. Thus, using the definition of the Hodge star, for any $\eta \in \wedge_2 \mathbb{R}^3$ we have

$$\begin{aligned} \eta \wedge [Q^{-T} \star Q^{-1} \xi] &= (Q^T \eta) \wedge [\star Q^{-1} \xi] \\ &= (Q^T \eta, Q^{-1} \xi)E \\ &= (\eta, \xi)E \\ &= \eta \wedge (\star \xi), \end{aligned}$$

and so $Q^{-T} \star Q^{-1} \xi = \star \xi$, completing the proof of the second equality in (A.12).

If we apply (A.10) with the α identified above to $w = q_1, q_2, q_3$ (which form a basis), then we obtain that the scaffold Q is transformed as

$$\begin{aligned} Q &\mapsto Q' := Q - (Qb)(\star v)^T Q \\ &= (\text{Id} - (Qb) \otimes (\star v)) Q \end{aligned}$$

at time t such that $(t, x) \in \text{supp } T^b(t)$. Also considering the multiplicity $\varphi^b(t) = m^b(t) = \|T^b(t)\|$ of the moving dislocations at time t and recalling that $\star v = N$ (the normal to H), we obtain (3.4).

A.6. Plastic flow. In this section we provide additional details concerning the derivation of the plastic flow equation (3.9). We start from (3.4), which means that from time t to $t + \delta$ we progress from Q to Q' given as

$$Q' := (\text{Id} - (Qb) \otimes [\star \mathbf{p}(S_\eta^b)((t, t + \delta) \times \Omega)]) Q.$$

Here we have set

$$\mathbf{p}(S_\eta^b) := \mathbf{p}(\vec{S}_\eta^b) \|S_\eta^b\| \in \mathcal{M}([0, T] \times \Omega; \Lambda_2 \mathbb{R}^3),$$

and we have used that locally around (t, x) we slip over the plane H with normal $N = \star v = \star \mathbf{p}(S_\eta^b(t, x))$ (we have already smeared out S^b via the dislocation line profile η) and with multiplicity $\|S_\eta^b\|$ (the ‘‘amount’’ of dislocations that flow).

In order to rewrite the above relation as a differential equation, we now need to identify the *density* of the measure on the right with respect to Lebesgue measure. We first observe $|\mathbf{p}(\vec{S}^b(t, x))| < 1$ for $\|S^b\|$ -almost every (t, x) . Otherwise, $\mathbf{p}(\vec{S}(t, x)) = \vec{S}(t, x)$ and there would exist a vertical piece in $\|S^b\|$, i.e., there would be a $t_0 \in [0, T]$ such that $\|S^b\|(\{t_0\} \times \mathbb{R}^3) > 0$, contradicting (A.7). So, by (A.8),

$$\nabla^{S^b} \mathbf{t}(t, x) \neq 0 \quad \text{for } \|S^b\| \text{-almost every } (t, x).$$

From the coarea formula for slices, see (A.4), we then get for any $\omega \in \mathcal{D}^2(\mathbb{R}^{1+3})$ that

$$\begin{aligned} \langle \mathbf{p}(S_\eta^b), \omega \rangle &= \int \langle \mathbf{p}(\vec{S}^b(t, x)), [\eta * \omega(t, \cdot)](x) \rangle d\|S^b\|(t, x) \\ &= \int_0^1 \int \left\langle \frac{\mathbf{p}(\vec{S}^b(t, x))}{|\nabla^{S^b} \mathbf{t}(t, x)|}, [\eta * \omega(t, \cdot)](x) \right\rangle d\|S^b|_t(x) dt \\ &= \int_0^1 \int \left\langle \eta * \left[\frac{\mathbf{p}(\vec{S}^b(t, \cdot)) \|S^b|_t\|}{|\nabla^{S^b} \mathbf{t}(t, \cdot)|} \right], \omega \right\rangle dx dt. \end{aligned} \tag{A.13}$$

The expression in the duality bracket on the right is thus the density of the measure $\mathbf{p}(S_\eta^b)$, which we call the (2-vector version of the) **geometric slip rate** $\gamma^b = \gamma^b(t, x) \in \Lambda_2 \mathbb{R}^3$ (for the Burgers vector $b \in \mathcal{B}$). Using also the definition of the dislocation velocity in (A.9),

$$\gamma^b(t, \cdot) = \eta * \left[\frac{D}{Dt} S^b(t, \cdot) \wedge \mathbf{p}(\vec{S}^b|_t) \|S^b|_t\| \right] = \eta * \left[\frac{D}{Dt} S^b(t, \cdot) \wedge T^b(t) \right],$$

which is (3.11).

The above arguments together with the definition $g^b := \star \gamma^b$ of the **normal slip rate** (called ‘‘geometric slip rate’’ in Section 3.3) give that in the time interval $[t, t + \delta]$ ($\delta > 0$) the scaffold Q changes to

$$Q' := \left(\text{Id} - (Qb) \otimes \int_t^{t+\delta} g^b(\tau) d\tau \right) Q.$$

Thus,

$$-Q(t)^{-1} \frac{Q(t+\delta) - Q(t)}{\delta} Q(t)^{-1} = b \otimes \frac{1}{\delta} \int_t^{t+\delta} g^b(\tau) d\tau$$

Letting $\delta \rightarrow 0$, we arrive at

$$\dot{P} = -Q^{-1} \dot{Q} Q^{-1} = b \otimes g^b(t).$$

It remains to integrate against the Burgers measure κ to take into account the slip for all Burgers vectors b to obtain the plastic flow equation (3.9) and the definition of the total plastic drift in (3.10).

A.7. Proof the consistency condition. To prove the consistency condition (3.12) at $t > 0$, we assume that this equation holds at $t = 0$ (as an initial condition) and then argue as follows: Recall the plastic flow equation (3.9) and (3.10), which read as

$$\dot{P} = \int b \otimes g^b \, d\kappa(b).$$

We integrate this in time from 0 to t and apply the row-wise curl $= \nabla \times$ (in space) to both sides, to obtain

$$\operatorname{curl} P(t) - \operatorname{curl} P(0) = \int b \otimes \left(\operatorname{curl} \int_0^t g^b(\tau) \, d\tau \right) \, d\kappa(b). \quad (\text{A.14})$$

To evaluate the right-hand side, we use that $g^b = \star \gamma^b$ and observe

$$\int_0^t g^b(\tau) \, d\tau = \int_0^t \star \gamma^b(\tau) \, d\tau = \star \int_0^t \gamma^b(\tau) \, d\tau = \star \mathbf{p}_*(S_\eta^b \lrcorner ((0, t) \times \Omega))$$

by similar arguments as in (A.13). Using that “ $\operatorname{curl} \circ \star = \partial$ ”, which will be shown below, as well as (A.3), (A.5), and $T_\eta^b(t) = \mathbf{p}_*(S_\eta^b|_t)$, we then obtain

$$\begin{aligned} \operatorname{curl} \int_0^t \star \gamma^b(\tau) \, d\tau &= \partial [\mathbf{p}_*(S_\eta^b \lrcorner ((0, t) \times \Omega))] \\ &= \mathbf{p}_* [\partial (S_\eta^b \lrcorner ((0, t) \times \Omega))] \\ &= \mathbf{p}_* [S_\eta^b|_t - S_\eta^b|_0] \\ &= T_\eta^b(t) - T_\eta^b(0). \end{aligned}$$

Note that we can only do this at t for which the slice $S_\eta^b|_t$ is defined, but this is the case almost everywhere in $(0, T)$. Plugging the last formula into (A.14),

$$\operatorname{curl} P(t) - \operatorname{curl} P(0) = \int b \otimes T_\eta^b(t) \, d\kappa(b) - \int b \otimes T_\eta^b(0) \, d\kappa(b).$$

Finally, using the consistency condition (3.12) at $t = 0$, we thus arrive at (3.12) for every t where the slice is defined.

It remains to show the identity “ $\operatorname{curl} \circ \star = \partial$ ”. To do so, we recall that the Hodge dual for a k -covector α satisfies

$$\star \alpha = (\star \alpha^\flat)^\sharp$$

with the musical isomorphisms $\flat: \Lambda^k V \rightarrow \Lambda_k V$ (“lowering an index”) and $\sharp: \Lambda_k V \rightarrow \Lambda^k V$ (“raising an index”), which are determined by

$$\langle \xi, \alpha \rangle = (\xi^\flat, \alpha) = (\xi, \alpha^\sharp), \quad \xi \in \Lambda_k V, \alpha \in \Lambda^k V.$$

Then, let $S \in I_2(\mathbb{R}^3)$ and compute, using $\operatorname{curl} v = (\star dv)^\sharp$, for any $\omega \in \mathcal{D}^1(\mathbb{R}^3)$ as follows:

$$\int \langle \operatorname{curl}(\star S), \omega \rangle = \int (\star S, \operatorname{curl}(\omega^\sharp)) = \int (\star S, (\star d\omega)^\sharp) = \int \langle S, d\omega \rangle = \int \langle \partial S, \omega \rangle,$$

which proves the claim.

REFERENCES

- [1] R. Abbaschian, L. Abbaschian, and R. E. Reed-Hill, *Physical Metallurgy Principles - SI Edition*, Cengage Learning, 2009.
- [2] A. Acharya, *Driving forces and boundary conditions in continuum dislocation mechanics*, Proc. R. Soc. London, Ser. A **459** (2003), 1343–1363.
- [3] ———, *Constitutive analysis of finite deformation field dislocation mechanics*, J. Mech. Phys. Solids **52** (2004), 301–316.
- [4] R. Alicandro, L. De Luca, A. Garroni, and M. Ponsiglione, *Metastability and dynamics of discrete topological singularities in two dimensions: a Γ -convergence approach*, Arch. Ration. Mech. Anal. **214** (2014), 269–330.
- [5] ———, *Minimising movements for the motion of discrete screw dislocations along glide directions*, Calc. Var. Partial Differential Equations **56** (2017), 87–104.
- [6] L. Ambrosio, N. Fusco, and D. Pallara, *Functions of Bounded Variation and Free-Discontinuity Problems*, Oxford Mathematical Monographs, Oxford University Press, 2000.
- [7] R. J. Amodeo and N. M. Ghoniem, *Dislocation dynamics. I. A proposed methodology for deformation micromechanics*, Phys. Rev. B **41** (1990), 6958–6967.
- [8] ———, *Dislocation dynamics. II. Applications to the formation of persistent slip bands, planar arrays, and dislocation cells*, Phys. Rev. B **41** (1990), 6968–6976.
- [9] P. M. Anderson, J. P. Hirth, and J. Lothe, *Theory of dislocations*, Cambridge University Press, 2017.
- [10] M. P. Ariza and M. Ortiz, *Discrete crystal elasticity and discrete dislocations in crystals*, Arch. Ration. Mech. Anal. **178** (2005), 149–226.
- [11] P. Ariza, S. Conti, A. Garroni, and M. Ortiz, *Variational modeling of dislocations in crystals in the line-tension limit*, European Congress of Mathematics, European Mathematical Society, 2018, pp. 583–598.
- [12] R. W. Armstrong, W. Arnold, and F. J. Zerilli, *Dislocation mechanics of copper and iron in high rate deformation tests*, J. Appl. Phys. **105** (2009), 023511.
- [13] E. Ben-David, T. Tepper-Faran, D. Rittel, and D. Shilo, *A large strain rate effect in thin free-standing Al films*, Scripta Materialia **90–91** (2014), 6–9.
- [14] B. A. Bilby, R. Bullough, and E. Smith, *Continuous distributions of dislocations: a new application of the methods of non-Riemannian geometry*, Proc. R. Soc. London, Ser. A **231** (1955), 263–273.
- [15] V. V. Bulatov and W. Cai, *Computer simulations of dislocations*, Oxford Series on Materials Modelling, vol. 3, Oxford University Press, 2006.
- [16] J. M. Burgers, *Some considerations on the fields of stress connected with dislocations in a regular crystal lattice. I.*, Proc. K. Ned. Akad. Wet. **42** (1939), 293–325.
- [17] ———, *Some considerations on the fields of stress connected with dislocations in a regular crystal lattice. II. Solutions of the equations of elasticity for a non-isotropic substance of regular crystalline symmetry*, Proc. K. Ned. Akad. Wet. **42** (1939), 378–399.
- [18] W. Cai, A. Arsenlis, C. R. Weinberger, and V. V. Bulatov, *A non-singular continuum theory of dislocations*, J. Mech. Phys. Solids **54** (2006), 561–587.
- [19] J. A. Carrillo, J. Mateu, M. G. Mora, L. Rondi, L. Scardia, and J. Verdera, *The ellipse law: Kirchhoff meets dislocations*, Comm. Math. Phys. **373** (2020), 507–524.
- [20] J. Casey and P. M. Naghdi, *A Remark on the Use of the Decomposition $F = FeFp$ in Plasticity*, J. Appl. Mech. **47** (1980), 672–675.
- [21] Ph. G. Ciarlet, *Mathematical Elasticity*, vol. 1: Three Dimensional Elasticity, North-Holland, 1988.
- [22] Ph. G. Ciarlet, L. Gratie, and C. Mardare, *Intrinsic methods in elasticity: a mathematical survey*, Discrete Contin. Dyn. Syst. **23** (2009), 133–164.
- [23] B. D. Coleman and W. Noll, *The thermodynamics of elastic materials with heat conduction and viscosity*, Arch. Ration. Mech. Anal. **13** (1963), 167–178.
- [24] S. Conti, A. Garroni, and A. Massaccesi, *Modeling of dislocations and relaxation of functionals on 1-currents with discrete multiplicity*, Calc. Var. Partial Differential Equations **54** (2015), 1847–1874.
- [25] S. Conti, A. Garroni, and M. Ortiz, *The line-tension approximation as the dilute limit of linear-elastic dislocations*, Arch. Ration. Mech. Anal. **218** (2015), 699–755.
- [26] S. Conti and F. Theil, *Single-Slip Elastoplastic Microstructures*, Arch. Ration. Mech. Anal. **178** (2005), 125–148.
- [27] Y. F. Dafalias, *Issues on the constitutive formulation at large elastoplastic deformations, part 1: Kinematics*, Acta Mech. **69** (1987), 119–138.
- [28] G. Dal Maso, A. DeSimone, and F. Solombrino, *Quasistatic evolution for Cam-Clay plasticity: a weak formulation via viscoplastic regularization and time rescaling*, Calc. Var. Partial Differential Equations **40** (2010), 125–181.
- [29] ———, *Quasistatic evolution for Cam-Clay plasticity: properties of the viscosity solution*, Calc. Var. Partial Differential Equations **44** (2011), 495–541.
- [30] T. M. De Hossony, A. Roos, and E. D. Metselaar, *Temperature rise due to fast-moving dislocations*, Philos. Mag. A **81** (2001), 1099–1120.

- [31] L. De Luca, A. Garroni, and M. Ponsiglione, Γ -convergence analysis of systems of edge dislocations: the self energy regime, *Arch. Ration. Mech. Anal.* **206** (2012), 885–910.
- [32] W. E and P. Ming, *Cauchy-Born rule and the stability of crystalline solids: dynamic problems*, *Acta Math. Appl. Sin. Engl. Ser.* **23** (2007), 529–550.
- [33] ———, *Cauchy-Born rule and the stability of crystalline solids: static problems*, *Arch. Ration. Mech. Anal.* **183** (2007), 241–297.
- [34] M. Epstein, *The geometrical language of continuum mechanics*, Cambridge University Press, 2010.
- [35] M. Epstein, R. Kupferman, and C. Maor, *Limits of distributed dislocations in geometric and constitutive paradigms*, *Geometric Continuum Mechanics* (R. Segev and M. Epstein, eds.), Birkhäuser, 2020.
- [36] J. L. Ericksen, *On the Cauchy-Born rule*, *Math. Mech. Solids* **13** (2008), 199–220.
- [37] H. Federer, *Geometric Measure Theory*, *Grundlehren der mathematischen Wissenschaften*, vol. 153, Springer, 1969.
- [38] G. A. Francfort and A. Mielke, *Existence results for a class of rate-independent material models with nonconvex elastic energies*, *J. Reine Angew. Math.* **595** (2006), 55–91.
- [39] M. Frémond, *Non-Smooth Thermomechanics*, Springer, 2002.
- [40] A. Garroni, G. Leoni, and M. Ponsiglione, *Gradient theory for plasticity via homogenization of discrete dislocations*, *J. Eur. Math. Soc. (JEMS)* **12** (2010), 1231–1266.
- [41] A. Garroni, P. van Meurs, M. A. Peletier, and L. Scardia, *Boundary-layer analysis of a pile-up of walls of edge dislocations at a lock*, *Math. Models Methods Appl. Sci.* **26** (2016), 2735–2768.
- [42] D. Grandi and U. Stefanelli, *Finite plasticity in $P^T P$. Part I: Constitutive model*, *Contin. Mech. Thermodyn.* **29** (2017), 97–116.
- [43] A. E. Green and P. M. Naghdi, *Some remarks on elastic-plastic deformation at finite strain*, *Internat. J. Engrg. Sci.* **9** (1971), 1219–1229.
- [44] M. E. Gurtin, *On the plasticity of single crystals: free energy, microforces, plastic-strain gradients*, *J. Mech. Phys. Solids* **48** (2000), 989–1036.
- [45] M. E. Gurtin, E. Fried, and L. Anand, *The Mechanics and Thermodynamics of Continua*, Cambridge University Press, 2010.
- [46] W. Han and B. D. Reddy, *Plasticity – Mathematical Theory and Numerical Analysis*, *Interdisciplinary Applied Mathematics*, vol. 9, Springer, 2013.
- [47] F. W. Hehl and Y. N. Obukhov, *Élie Cartan’s torsion in geometry and in field theory, an essay*, *Ann. Fond. Louis de Broglie* **32** (2007), 157–194.
- [48] T. Hochrainer, S. Sandfeld, M. Zaiser, and P. Gumbsch, *Continuum dislocation dynamics: Towards a physical theory of crystal plasticity*, *J. Mech. Phys. Solids* **63** (2014), 167–178.
- [49] T. Hochrainer, M. Zaiser, and P. Gumbsch, *A three-dimensional continuum theory of dislocation systems: kinematics and mean-field formulation*, *Philos. Mag.* **87** (2007), 1261–1282.
- [50] T. Hudson, *Upscaling a model for the thermally-driven motion of screw dislocations*, *Arch. Ration. Mech. Anal.* **224** (2017), 291–352.
- [51] T. Hudson and C. Ortner, *On the stability of Bravais lattices and their Cauchy-Born approximations*, *ESAIM Math. Model. Numer. Anal.* **46** (2012), 81–110.
- [52] ———, *Existence and stability of a screw dislocation under anti-plane deformation*, *Arch. Ration. Mech. Anal.* **213** (2014), 887–929.
- [53] ———, *Analysis of stable screw dislocation configurations in an antiplane lattice model*, *SIAM J. Math. Anal.* **47** (2015), 291–320.
- [54] T. Hudson, P. van Meurs, and M. A. Peletier, *Atomistic origins of continuum dislocation dynamics*, *Math. Models Methods Appl. Sci.* **30** (2020), 2557–2618.
- [55] D. Hull and D. J. Bacon, *Introduction to Dislocations*, 5 ed., Elsevier, 2011.
- [56] M. E. Kassner, P. Geantil, L. E. Levine, and B. C. Larson, *Backstress, the Bauschinger effect and cyclic deformation*, *Mater. Sci. Forum* **604–605** (2009), 39–51.
- [57] M. O. Katanaev, *Geometric theory of defects*, *Phys. Usp.* (2005), 675–701.
- [58] S. G. Krantz and H. R. Parks, *Geometric integration theory*, Birkhäuser, 2008.
- [59] E. Kröner, *Allgemeine Kontinuumstheorie der Versetzungen und Eigenspannungen*, *Arch. Ration. Mech. Anal.* **4** (1960), 273–334.
- [60] E. Kröner, *Bemerkung zum geometrischen Grundgesetz der allgemeinen Kontinuumstheorie der Versetzung und Eigenspannungen*, *Arch. Ration. Mech. Anal.* **7** (1961), 78–80.
- [61] ———, *Benefits and shortcomings of the continuous theory of dislocations*, *Int. J. Solids Struct.* **38** (2001), 1115–1134.
- [62] E. Kröner and A. Seeger, *Nicht-lineare Elastizitätstheorie der Versetzungen und Eigenspannungen*, *Arch. Ration. Mech. Anal.* **3** (1959), 97–119.
- [63] R. Kupferman and C. Maor, *The emergence of torsion in the continuum limit of distributed edge-dislocations*, *J. Geom. Mech.* **7** (2015), 361–387.

- [64] R. Kupferman and E. Olami, *Homogenization of edge-dislocations as a weak limit of de-Rham currents*, Geometric Continuum Mechanics (R. Segev and M. Epstein, eds.), Birkhäuser, 2020.
- [65] M. Lazar, *Dislocation theory as a 3-dimensional translation gauge theory*, Ann. Phys. **9** (2000), 461–473.
- [66] M. Lazar and C. Anastassiadis, *The gauge theory of dislocations: conservation and balance laws*, Philos. Mag. **88** (2008), 1673–1699.
- [67] ———, *The gauge theory of dislocations: Static solutions of screw and edge dislocations*, Philos. Mag. **89** (2009), 199–231.
- [68] E. H. Lee, *Elastic-plastic deformation at finite strain*, ASME J. Appl. Mech. **36** (1969), 1–6.
- [69] E. H. Lee and D. T. Liu, *Finite-strain elastic-plastic theory with application to plane-wave analysis*, J. Appl. Phys. **38** (1967), 19–27.
- [70] J. Lemaitre and J.-L. Chaboche, *Mechanics of solid materials*, Cambridge University Press, 1990.
- [71] M. Lewicka and M. R. Pakzad, *Scaling laws for non-Euclidean plates and the $W^{2,2}$ isometric immersions of Riemannian metrics*, ESAIM Control Optim. Calc. Var. **17** (2011), 1158–1173.
- [72] V. A. Lubarda and E. H. Lee, *A Correct Definition of Elastic and Plastic Deformation and Its Computational Significance*, J. Appl. Mech. **48** (1981), 35, Erratum: J. Appl. Mech. **48** (1981), 686.
- [73] J. Lubliner, *Plasticity Theory*, Dover, 2008.
- [74] A. Mainik and A. Mielke, *Existence results for energetic models for rate-independent systems*, Calc. Var. Partial Differential Equations **22** (2005), 73–99.
- [75] ———, *Global existence for rate-independent gradient plasticity at finite strain*, J. Nonlinear Sci. **19** (2009), 221–248.
- [76] C. Malyshev, *The Einsteinian $T(3)$ -gauge approach and the stress tensor of the screw dislocation in the second order: avoiding the cut-off at the core*, J. Phys. A **40** (2007), 10657–10684.
- [77] J. Mandel, *Equations constitutives et directeurs dans les milieux plastiques et viscoplastiques*, Int. J. Solids Struct. **9** (1973), 725–740.
- [78] A. Mielke, *Finite elastoplasticity Lie groups and geodesics on $SL(d)$* , Geometry, mechanics, and dynamics, Springer, 2002, pp. 61–90.
- [79] ———, *Energetic formulation of multiplicative elasto-plasticity using dissipation distances*, Contin. Mech. Thermodyn. **15** (2003), 351–382.
- [80] A. Mielke and S. Müller, *Lower semicontinuity and existence of minimizers in incremental finite-strain elastoplasticity*, ZAMM Z. Angew. Math. Mech. **86** (2006), 233–250.
- [81] A. Mielke, R. Rossi, and G. Savaré, *Modeling solutions with jumps for rate-independent systems on metric spaces*, Discrete Contin. Dyn. Syst. **25** (2009), 585–615.
- [82] ———, *BV solutions and viscosity approximations of rate-independent systems*, ESAIM Control Optim. Calc. Var. **18** (2012), 36–80.
- [83] A. Mielke and T. Roubíček, *Rate-Independent Systems: Theory and Application.*, Applied Mathematical Sciences, vol. 193, Springer, 2015.
- [84] S. Müller, L. Scardia, and C. I. Zeppieri, *Geometric rigidity for incompatible fields, and an application to strain-gradient plasticity*, Indiana Univ. Math. J. **63** (2014), 1365–1396.
- [85] P. M. Naghdi, *A critical review of the state of finite plasticity*, Z. Angew. Math. Phys. **41** (1990), 315–394.
- [86] S. Nemat-Nasser, *Decomposition of strain measures and their rates in finite deformation elastoplasticity*, Int. J. Solids Struct. **15** (1979), 155–166.
- [87] J. F. Nye, *Some geometrical relations in dislocated crystals*, Acta Metall. **1** (1953), 153–162.
- [88] M. Ortiz and E. A. Repetto, *Nonconvex energy minimization and dislocation structures in ductile single crystals*, J. Mech. Phys. Solids **47** (1999), 397–462.
- [89] C. Ortner and F. Theil, *Justification of the Cauchy-Born approximation of elastodynamics*, Arch. Ration. Mech. Anal. **207** (2013), 1025–1073.
- [90] M. Peach and J. S. Koehler, *The forces exerted on dislocations and the stress fields produced by them*, Phys. Rev. **80** (1950), 436–439.
- [91] M. Ponsiglione, *Elastic energy stored in a crystal induced by screw dislocations: from discrete to continuous*, SIAM J. Math. Anal. **39** (2007), 449–469.
- [92] C. Reina and S. Conti, *Kinematic description of crystal plasticity in the finite kinematic framework: A micromechanical understanding of $F=FeFp$* , J. Mech. Phys. Solids **67** (2014), 40–61.
- [93] C. Reina, L. F. Djodom, M. Ortiz, and S. Conti, *Kinematics of elasto-plasticity: validity and limits of applicability of $\mathbf{F} = \mathbf{F}^e \mathbf{F}^p$ for general three-dimensional deformations*, J. Mech. Phys. Solids **121** (2018), 99–113.
- [94] J. R. Rice, *Inelastic constitutive relations for solids: An internal-variable theory and its application to metal plasticity*, J. Mech. Phys. Solids **19** (1971), 433–455.
- [95] F. Rindler, *Energetic solutions to rate-independent large-strain elasto-plastic evolutions driven by discrete dislocation flow*, Preprint.
- [96] ———, *Space-time integral currents of bounded variation*, Preprint.
- [97] ———, *A two-speed model for finite-strain elasto-plasticity*, arXiv:1512.05928.

- [98] F. Rindler, S. Schwarzacher, and J. J. L. Velazquez, *Two-speed solutions to non-convex rate-independent systems*, Arch. Ration. Mech. Anal. **239** (2021), 1667–1731.
- [99] R. T. Rockafellar, *Convex Analysis*, Princeton Mathematical Series, vol. 28, Princeton University Press, 1970.
- [100] S. Sandfeld, T. Hochrainer, M. Zaiser, and P. Gumbsch, *Continuum modeling of dislocation plasticity: Theory, numerical implementation, and validation by discrete dislocation simulations*, J. Mater. Res. **26** (2011), 623–632.
- [101] R. Scala and N. Van Goethem, *Variational evolution of dislocations in single crystals*, J. Nonlinear Sci. **29** (2019), 319–344.
- [102] L. Scardia, R. H. J. Peerlings, M. A. Peletier, and M. G. D. Geers, *Mechanics of dislocation pile-ups: a unification of scaling regimes*, J. Mech. Phys. Solids **70** (2014), 42–61.
- [103] M. Silhavy, *The Mechanics and Thermodynamics of Continuous Media*, Springer, 1997.
- [104] U. Stefanelli, *A Variational Principle for Hardening Elastoplasticity*, SIAM J. Math. Anal. **40** (2008), 623–652.
- [105] R. Temam, *Mathematical problems in plasticity*, Dover, 2018.
- [106] E. van der Giessen and A. Needleman, *Discrete dislocation plasticity: a simple planar model*, Handbook of Materials Modeling, Springer, 1995, pp. 689–735.
- [107] P. van Meurs, A. Muntean, and M. A. Peletier, *Upscaling of dislocation walls in finite domains*, European J. Appl. Math. **25** (2014), 749–781.
- [108] L. D. Williams, *Geometric Rigidity and an Application to Statistical Mechanics*, Ph.D. thesis, University of Warwick, 2017.
- [109] H. M. Zbib, *On the mechanics of large inelastic deformations: kinematics and constitutive modeling*, Acta Mech. **96** (1993), 119–138.
- [110] H. Ziegler and C. Wehrli, *The derivation of constitutive relations from the free energy and the dissipation function*, Advances in applied mechanics, Vol. 25, Adv. Appl. Mech., vol. 25, Academic Press, 1987, pp. 183–237.

MATHEMATICS INSTITUTE, UNIVERSITY OF WARWICK, COVENTRY CV4 7AL, UNITED KINGDOM.
Email address: F.Rindler@warwick.ac.uk